Design and Experimental Validation of Longitudinal Controller of Connected Vehicles using Model Predictive Control

by

Xiaolong Cao

A thesis submitted to the Graduate Faculty of
Auburn University
in partial fulfillment of the
requirements for the Degree of
Master of Science

Auburn, Alabama
December 12, 2015

Keywords: Connected Vehicle, Laguerre functions, vehicle following, Vehicle-to-Vehicle Communication, DSRC, Model Predictive Control, MicroAutoBox

Approved by

David Bevly, Chair, Professor of Mechanical Engineering
George Flowers, Professor of Mechanical Engineering
John Hung, Professor of Electrical Engineering

Abstract

In this thesis, a vehicle longitudinal control algorithm based on model predictive control (MPC) is applied to compute the desired relative acceleration of the following vehicle in leader-follower systems. Kinematic equations are used to describe the dynamic relationship between the leading and following vehicles. Compared to the conventional model predictive control (CMPC), the control horizon is expressed using Laguerre functions. This makes the optimization problem easier to solve and available to be tuned. Appropriate parameters are investigated by comparing the different approximation results under different decay factors. The design of MPC based on Laguerre functions (LMPC) enables the system to be adjustable through the selection of the decay factors depending on the characteristics such as response time and overshoot of the closed-loop system. The effectiveness of the design approach was demonstrated using simulations and experiments. Control performance of the closed-loop system was investigated by selecting different parameters including the states weighting matrix, the input weighting matrix, and Laguerre coefficients. With constraints on the control variables and the difference of the control variables, the following vehicle can track the leading vehicle with a specific distance and at the same speed in the simulation. Experiments which illustrate the performance of the control system were performed on an experimental platform used by Federal Highway Administration (FHWA), followed by the experimental data showing the following vehicle can track the leading vehicle with a specific distance and at the same speed. However, there is overshoot of the distance and the relative speed is not zero. The reasons of the poor performance of the control system were explored, which include the absence of the acceleration of the leading vehicle, large constraints on the difference of the desired acceleration. Solutions such as decreasing the constraints on the incremental variation and enlarging the input weighting matrix are discussed.

Acknowledgments

This work could only have been carried out with the kind assistance of colleagues, family and friends. I would like to thank my supervisor Dr. Bevly for his support and guidance throughout this project. I was fortunate to be able to absorb from his skills, not only in the control theory and research in the field, but also his knowledge of the English language and his precision. I am also indebted to the other members of my examination committee Prof. John Hung and Prof. George Flowers for their assessment of my thesis and research.

I also owe much to my fellow students. Tong was especially helpful when I first began and each frequently offered their own time to help me with this or that. To the GAVLAB members, thank you for the technical discussions. To Lowell Brown, for the help and assistance. Thanks to Yan for discussions on the control theory. Thank you to those who reviewed and made comments on the thesis as well.

I wish to thank Federal Highway Administration for sponsoring this work and giving me the opportunity to come to Washington, D.C. for the summer. It was an invaluable experience, and I enjoyed meeting all of the good people up there. Special thanks goes to Guchan and Petrick for their involvement in this work and all of the assistance they provided.

Finally, I would now like to acknowledge my parents, who have been encoring and supportive throughout my entire life. There is no doubt that I would not be where I am today with out them. Likewise I want to thank my three sisters for their constant love and support, for always being there, and for always encouraging me to do my best, something which they have each modeled with great integrity.

Table of Contents

Abstract ii

Acknowledgments iii

List of Figures vi

List of Tables viii

1 Introduction and Background 1

1.1 Prior Research 3

1.2 Contributions 9

2 Longitudinal Model for Vehicle Following 12

2.1 Problem Statement 12

2.2 System Modeling 13

2.2.1 Augmented Model for Model Predictive Control 13

2.2.2 Vehicle Following Model 15

2.3 Conclusion 16

3 Controller Design based on Model Predictive Control 17

3.1 Introduction 17

3.2 Basic Idea of Model Predictive Control 17

3.3 Optimization of Incremental Control using Laguerre Functions 19

3.3.1 Discrete-time Laguerre Networks 19

3.3.2 Minimization of Cost Function 23

3.4 Constraints 28

3.4.1 Test of TORC Speed Controller 28

3.5 Use of Laguerre Functions as Tuning Parameters 30

3.6 Conclusion 33

4 Experimental Validation 35
4.1 Introduction 35
4.2 System Architecture 35
4.3 Hardwares Descriptions 36
4.3.1 PinPoint Localization Module 36
4.3.2 DSRC Onboard Equipment (OBE) 38
4.3.3 MicroAutobox II 39
4.3.4 TORC Automotive Interface Module 40
4.4 Software Setup 41
4.5 Experimental Results 42
4.5.1 Test of Vehicle Following Controller 42
4.6 Discussion of Experimental Data 45
4.6.1 Absence of the Acceleration of Leading Vehicle 45
4.6.2 Constraints on the Difference of Control Variable 47
4.7 Conclusion 52
5 Conclusion and Future work 53
Bibliography 55
Appendices 60
A Notes on the style-file project 61

List of Figures

1.1 Framework of intelligent vehicle [34] 3

2.1 Vehicle Following, X represents position and V represents velocity [6] 12

3.1 Discrete Laguerre network 20

3.2 Approximation to the Impulse Response ($a = 0.3$) 22

3.3 Approximation to the Impulse Response ($a = 0.6$) 22

3.4 Approximation to the Impulse Response ($a = 0.9$) 23

3.5 Step Change in Set Speed of the TORC Speed Controller 29

3.6 Distance between Leader and Follower 32

3.7 Relative Speed between Leader and Follower 32

4.1 System Infrastructure 36

4.2 Experimental setup in the vehicle which includes MicroAutoBox, DSRC and PinPoint 37

4.3 Cadillac SRX used for the experimental test 37

4.4 PinPoint 38

4.5 Positions from PinPoint 39

4.6 DSRC 39

4.7 MicroAutoBox [7] 40

4.8 TORC Quad CAN ECU Module 41

4.9 User Interface of ControlDesk 42

4.10 Simulink Blocks of Controller Implementation 44

4.11 Actual Distance 45

4.12 Speed Comparison 45

4.13 Relative Speed 46

4.14 Control Switch 46

4.15 Desired Acceleration in the Test 48

4.16 Distance 49

4.17 Relative Speed 49

4.18 Desired Relative Acceleration 50

4.19 Distance 50

4.20 Relative Speed 51

4.21 Desired Relative Acceleration 51

4.22 Incremental Variation of the Desired Relative Acceleration 52

List of Tables

3.1 Discrete Eigenvalues of Closed-loop System of different decay factors (a) 31

3.2 Feedback gain of Closed-loop System of different decay factors (a) 31

Chapter 1

Introduction and Background

Driving has been a commonplace aspect of modern society. However, many unintentional injuries and deaths have been caused by vehicle accidents [14]. There were 30,800 fatal car crashes in 2012 alone [15]. Researchers have been working on different driver assistance systems such as Adaptive Cruise Control (ACC) and Blind Spot Detection. ACC functionality is well known and available in many passenger cars and trucks today which has yielded increased safety, better fuel economy and more efficient traffic flow [16]. ACC is an optional cruise control system that automatically adjusts the vehicle speed to maintain a safe distance from the vehicle ahead for ground vehicles [17]. Commonly, a radar system is used to measure the distance and the relative velocity between the vehicles [22].

As vehicle automated following has become realized, applicable topics like automated lane change and merge and driverless vehicle have been explored by researchers. The radar system is not enough for the self-driving capabilities like automated lane change. With the development of wireless communication, the concept of connected vehicle (Vehicle-to-Vehicle Communication (V2V)) has been determined as the next step moving forward. Connected vehicle technology enables vehicles to have the ability to share vehicle information including position, velocity and other important navigation related information with other surrounding vehicles. V2V communication is implemented by Dedicated Short Range Communications (DSRC), leading to Cooperative Adaptive Cruise Control (CACC). Compared to the radar system, V2V communication has the following characteristics: fast network acquisition, high reliability [21] and higher accuracy. Additionally, data can be collected by the host vehicle to help the vehicle make decisions, such as accelerate or decelerate, lane change or not. With the concept of connected vehicles enabled by DSRC, a sequence of research activities was

initiated to evaluate vehicle safety applications like automated vehicle following by relying on V2V communication. However, how to integrate the DSRC with the other support systems including advanced positioning system and the control system, was the key point for the research, and the goal of this thesis.

When the vehicles have the ability to communicate with each other through DSRC, decisions (i.e. to command acceleration to accelerate or not in longitudinal control and to execute a lane change command or not in lateral control) made by control algorithms or control logic is the final step of the automated system. The framework of intelligent vehicle is shown in Figure 1.1, which is structured as a higher level controller and lower level controller. The higher level controller is the brain of the system, which could achieve some sophisticated tasks, such as decision making according to the traffic situation and the environment information. For vehicle following behavior, desired velocity of host vehicle can be calculated by higher level controller, which can maintain the desired gap and relative speed between the leading vehicles and following vehicles. For lane changing behavior, the value of desired yaw and steering angle can be given by the high level, which can implement automated lane change. The outputs from the higher level controller is sent to the lower controller, which is essentially comprised for a throttle/brake controller that regulates the speed and a steering controller that regulates the lateral displacement and yaw rate.

In this thesis, the focus is on the automated car following behavior implemented using DSRC. The TORC speed controller is the default lower controller shown in Figure 4.8. A higher level controller based on model predictive control is explored in this work. For the higher level controller, different control methods such as fuzzy logic-based controller [18], MPC [19] [22], PID controller [20], and PD controller [23] are applied for calculating the desired acceleration. In the next section, prior research about different control methods is discussed.

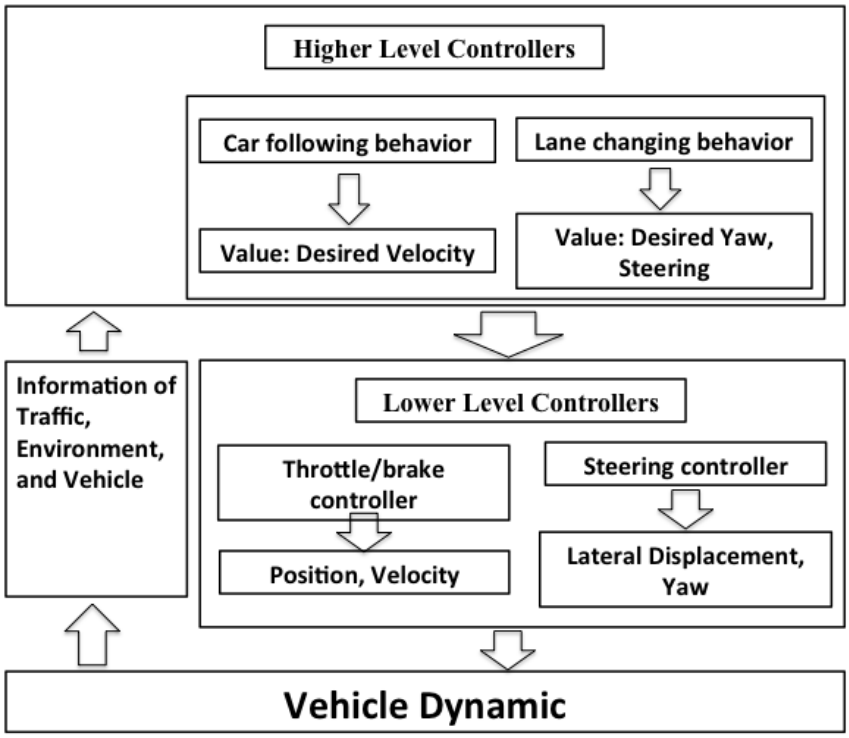

Figure 1.1: Framework of intelligent vehicle [34]

1.1 Prior Research

A considerable number of models or control methods are proposed in the literature. An Intelligent-Driver Model (IDM) is proposed in [35]. More specifically, the IDM is a car-following model. The decision to accelerate or to brake depends on the speed of host vehicle and on the position and speed of the leading vehicle immediately ahead. The IDM model equations are expressed as below:

$$\frac{dv}{dt} = a[1 - (\frac{v}{v_0})^{\delta} - (\frac{s^*(v, \Delta v)}{s})^2] \tag{1.1}$$

$$s^*(v, \Delta v) = s_0 + max[0, (vT + \frac{v\Delta v}{2\sqrt{ab}})] \tag{1.2}$$

where v_0 is desired speed when driving on a free road, T is desired safety time headway when following other vehicles, a is the acceleration of everyday traffic, b is the comfortable braking deceleration in everyday traffic, s_0 is the minimum bumper-to-bumper distance to the front vehicle, and δ is the acceleration component. The desired acceleration is given by the model represented by Equation (1.1) and Equation (1.2) . The model parameters describe the driving style such as slow or fast, careful or reckless.

A PID controller designed in [20], used the control law given by

$$u(t) = k_p e_v(t) + k_i \int e_v(t)d(t) + k_d \frac{de_v(t)}{dt} \tag{1.3}$$

where $e_v(t)$ is the deviation between the actual speed and the command speed, k_p, k_i and k_d are the coefficients of proportional, integral and derivative gains. The input $u(t)$ is the control input of the lower controller. Note this control algorithm just considers the speed error. The most commonplace PID controller will take into account the velocity error and the position error at the same time resulting from the control objective to maintain the distance and the relative speed. In this case, the control law for a PI controller is generally given by

$$u(t) = k_{p1} e_v(t) + k_{p2} e_d + k_{i1} \int e_v(t)d(t) + k_{i2} \int e_d(t)d(t) + k_a e_a \tag{1.4}$$

where e_d is the deviation between the actual gap and the desired gap, k_{p1}, k_a and k_{p2} denote the coefficients of the proportional terms, k_{i1} and k_{i2} are the coefficients of the integral term, and e_a is the acceleration error between the host vehicle and target vehicle.

The use of the terms e_v and e_d in the integral part is found in [36]. The primary benefit for including the time varying proportional terms is the reduction of the speed overshoot due to a large position error. But, in most of the literature, only a proportional action over the distance error, acceleration error and velocity error are considered [37], [38], [39], [41].

All the coefficients of proportional or integral terms should be determined considering the influence of the distance error and speed error.

Furthermore, a fuzzy logic-based controller is also widely explored considering a trade-off between a proper car-following gap error and the smoothness of the control signal[18], [40], [41], [42]. A fuzzy logic controller is a set of rules describing a set of actions to be taken for given inputs such as distance error and speed error without using a conventional, mathematical model. An example of the fuzzy logic rule is designed in [45]. GapError represents the error between the actual inter-vehicle distance with respect to the desired distance in meters, and its derivative $d_{GapError}$, permitting faster responses to vehicle changes. The crisp numeric values are transformed into linguistic values. Five fuzzy subsets called Negative Big (NB), Negative Medium (NM), Negative Small (NS), Zero Error (ZE), Positive Small (PS),Positive Medium (PM), and Positive Big (PB) are used as linguistic variables. The final output is computed by the inference engine. The linguistic values will be defuzzified and transformed into crisp values of desired speed.

Although the fuzzy logic controller is designed in these works [18], [40], [41], [42], there are still some differences between each other. A cost function is incorporated in the fuzzy logic-based controller. The controller is tuned to minimize a cost function in order to obtain a tradeoff between a proper car-following gap error and the smoothness of the control signal [18]. In [41], a sophisticated algorithm is applied to smooth the output for controlling the throttle and brake actuator. The packet delay ratio, delay and throughput of V2V communication are considered in the design of the fuzzy control system [41]. The maximum of the performance of a fuzzy logic controller is found using a genetic algorithm.

The CACC system is classified as a smart system. It takes advantage of the communication link to have access to the leading vehicle's position, speed and acceleration information. The vehicles equipped with CACC systems can track the other vehicle with a desired distance and at the same speed. Meanwhile, ride comfort of passengers, fuel savings, and the traffic flow are considered. To account for different characteristics, the MPC approach is

appropriate choice because it can use different constraint satisfactions. For conventional control methods like a PID controller, the outputs have to be limited to obey the minimum acceleration or minimum distance when the acceleration and distance are bounded. Because MPC is able to anticipate future situations and to implement constraints directly into the control algorithm, it is appears to be more promising than a PID control and fuzzy logic controllers. Minimal tracking error, low fuel consumption, and driver dynamic car-following characteristics can be considered in the quadratic cost function. The ride comfort, driver permissible tracking range and safe distance are formulated as linear constraints in [43]. However, these objectives usually conflict with each other. For instance, the improvement of the tracking capability increases the fuel consumption. If the system possesses better tracking capability, it leads to unnecessary acceleration and deceleration. Current state of the art suggest the MPC approach to be promising to comprehensively deal with different objectives simultaneously.

MPC applies the first input of a control sequence that optimizes a performance index calculated from predicted system behavior based on a prediction model in a receding horizon approach [1]. The controller is designed to control the acceleration of the following vehicle subject to operational constraints on acceleration. The MPC-based controller at each time step minimizes the expected errors in position and velocity and the corresponding input variation. Bageshwar *et al.* developed an MPC which is used for computing the spacing-control laws for transitional maneuvers [26] . A transitional maneuver is defined as a switch from ACC to Cruise Control (CC) and vice verse. For example, a transition from ACC to CC would occur if the leading vehicle disappear. The spacing-control laws based on MPC are obtained by solving the constrained optimal control problem using a receding-horizon approach, where the desired acceleration is computed at each sampling instant. The standard constant time gap algorithm is unable to perform the transitional maneuvers [26]. Feyyaz *et al.* demonstrates a model predictive controller with PID structure, which is able to accommodate actuator limits and parameter estimation [25] . Two different MPC models

are used in the system. When the the distance between the vehicles is less than 10 meters, a following MPC model with six states considering a rear-end check is activated. Otherwise, a four state model considering a preceding vehicle collision check is used.

Different parameterization methodologies have been investigated. A systematic approach to the design and tuning based on model predictive control was presented in [22]. The parameterization is a unique feature of the synthesized ACC. The system is available to be tuned considering the safety, comfort, and fuel economy. The methodology is to change the weights in the minimization function directly [22]. Implementation and performance evaluation of explicit MPC are presented in [11]. When a multi-parametric quadratic program with parameter vector is used as the cost function, the performance of the controller is available to be tuned depending on requirements by selecting different decay factors. The tuning method still attempts to change the weights in the cost function directly. Hybrid model predictive control system has also been used to solve a control problem for the tracking of a vehicle[27]. The controller aims to track the velocity transmitted by the leading vehicle. The control law in [27] is divided into two phases: tracking is considered during the transient of the reference trajectory and stability is the goal after the reference reaches its steady state using the hybrid MPC in the regulation. Also, robust MPC is discussed with the presence of disturbances which are approximated by piecewise affine systems.

Laguerre functions-based MPC (LMPC) is developed in [47, 54]. Laguerre functions are a set of orthonormal functions. When the control trajectory ΔU is expressed using Laguerre functions, the predictive control problem is reformulated and the solution is simplified. Laguerre functions have many advantages such as good approximation capability for different systems, low computational complexity, and better feasibility. For, large-scale systems, the optimization problem may be computationally intractable due to the large number of variables and the complexity of the constraints [47]. The system is difficult to implement in hardware with limited memory or low processing power required for the high online computational costs. It has been shown that LMPC reduces the computational complexity and

provides better feasibility then CMPC [53], [54]. Examples are given to show that LMPC gives better performance and feasibility than CMPC. At the same time, the loss of performance is negligible enough to ignore [48]. A novel mechanism is given to demonstrate the performance and feasibility benefits with respect to CMPC. The algorithm outperforms a conventional dual mode algorithm by giving substantially better feasibility with little compromise to performance [49], [52]. The design objectives such as feasibility, performance, and computational cost are conflicted. A multi objective evolutionary algorithm is given to obtain a suitable balance between feasibility, performance, and computational cost [54].

Moreover, some experiments have been done to validate the automatic vehicle following. Field tests of a Cooperative Adaptive Cruise Control (CACC) on real vehicles was carried out by California Partners for Advanced Transportation Technology (PATH) in United States using two Infinity FX45s [31]. In 2014, the researchers also successfully implemented a CACC system in four production Infinity M56s [33]. DSRC was used for wireless communication and MPC-based controller was designed as the gap regulation controller. The results showed that the time gaps of CACC are shorter than ACC, which will significantly increase the highway capacity in the future. At the same time, a control system was implemented on a test fleet consisting of six Toyota Prius in the Netherlands. CACC allows time gaps significantly smaller than 1s (0.7s) while maintaining string stability. As result, road throughput is increased and fuel consumption and emissions are decreased as expected [32]. Three different control strategies are designed depending on three driving situations which include safe, warning and dangerous mode for the vehicle following scenario in [24]. The test vehicle is equipped with a laser radar, accelerometers, ESC module, wheel speed sensors and wheel pressure sensors. The higher and lower level controllers are implemented by dSpace hardware (MicroAutoBox), which is also used in this work. However in this thesis, the distance is calculated by the vehicle information received through V2V communication not the radar system.

1.2 Contributions

The goal of this work is to design a control system based on model predictive control and implement the control system in MicroAutoBox. The distance and relative speed in leader-follower system is maintained to a pre-set value by controlling the speed of the following vehicle. The communication system (DSRC), positioning system (PinPoint), and control system (MicroAutobox) are introduced. Compared to the conventional solution methodology, the control trajectory is expressed by Laguerre functions. The results of approximating the impulse response of the system are presented. Different parameters including the number of network terms (N) and decay factor (a) are determined from simulations. This modification allows the closed-loop system to be tuned via the adjustment of different decay factors. Additionally, this work shows the capability of using V2V communication to share vehicle information consisting of position and velocity with the surrounding vehicles. Compared to the conventional ACC using radar to detect the distance between the vehicles, V2V communication improve the efficiency and precision of distance and speed detection. The following are the contributions contained in this thesis:

- An augmented model is developed for model predictive control based on the kinematic relationship between following and leading vehicles (initial results presented by Gerrit *et al.* in [11]).
- Coefficients of Laguerre functions were determined by simulations.
- Performance of Laguerre functions based MPC (LMPC) are compared depending on different decay factors with the constraints of control variables.
- The concept of connected vehicles and LMPC control algorithm are experimental validated and future improvements of the control system are discussed.

The first contribution of this work is the development of an augmented model specifically used for MPC. The model is originally based on kinematic equations which is a well known

car-following model used in [11], [12]. The states are distance between the two vehicles and relative speed. According to the model predictive control theory presented in this thesis, the other two states are the error of distance and the error of the relative speed. Therefore, the augmented model has four states. The objective of the controller is to maintain a pre-set distance and a zero relative speed between the leading and following vehicles.

Laguerre functions are used to approximate the transfer function model of a physical system. Different approximation results are presented depending on the different parameters of the Laguerre functions. In the time domain, the Laguerre functions are polynomials multiplied by a decaying exponential [13]. This property is very significant when it is used for describing the control horizon in MPC. Namely, the system with Laguerre functions is tunable via adjustment of several parameters. Additionally, for some large scale system, it has other advantages such as low computational cost and better feasibility. Unique to Laguerre formulation, suitable parameters are needed to describe the control horizon from the simulation results.

Laguerre functions are a set of exponential functions with a decay factor. When the control horizon is described by Laguerre functions, the incremental control signal is a forced exponentially decay [8]. More emphasis is placed on the control trajectory at the current time and less emphasis on those at future times while the sampling instant increases in the cost function. The closed-loop control performance is affected by decay factor of Laguerre functions. This is particularly useful when the CMPC can not provide satisfactory performance. The LMPC provides additional methods for fine tuning the closed-loop performance such as stability, response time, and overshoot.

The final contribution is the experimental implementation of the concept of the connected vehicles. In the experiments, PinPoint, which is a combination of GPS and IMU (Inertial Measurement Unit), provides the navigation and localization information such as position and velocity. DSRC (Dedicated Short Range Communication) is used as the V2V

communication which makes it possible for the vehicles to share messages with the surrounding vehicles. Accordingly, the distance and relative speed are calculated directly from the individual vehicle measurement instead of the radar measurements. The MicroAutoBox is responsible for implementing the control algorithm developed in Simulink, as it is much easier to change parameters such as speed command and desired distance through the interface of ControlDesk.

Chapter 2

Longitudinal Model for Vehicle Following

2.1 Problem Statement

A maneuver called automated following is the most common application for connected vehicles. A schematic representation of vehicle following is shown in Figure 2.1. Focusing on the design of the vehicle following control system, a model which can provide the longitudinal relative dynamics in a vehicle following scenario is needed. Basically, the longitudinal control consists of higher and lower control levels as discussed before. The higher level is a supervisory controller that governs the desired distance and speed to maintain the distance and relative speed between the two vehicles. The low-level controller is essentially a throttle/brake controller that regulates the desired speed. The focus of this thesis is on the design of higher level controller.

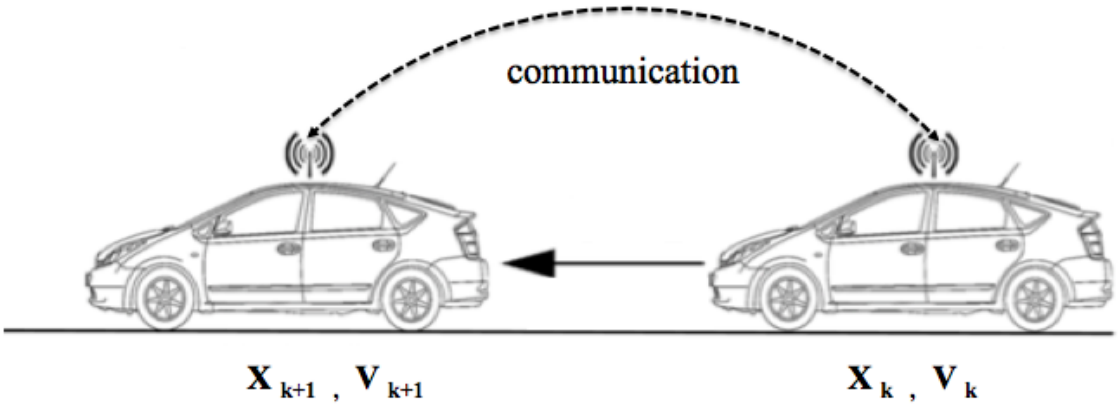

Figure 2.1: Vehicle Following, X represents position and V represents velocity [6]

2.2 System Modeling

2.2.1 Augmented Model for Model Predictive Control

The formulation of MPC below is referenced primarily from [5]. Assuming that the plant has m inputs, q outputs and n_1 states and $q \leq m$. The system is described by

$$x(k+1) = Ax(k) + Bu(k) \tag{2.1}$$

$$y(k) = Cx(k) \tag{2.2}$$

where x denotes the state variable with assumed dimension n_1; u is the input variable with assumed dimension m; y is the process output with assumed dimension q. In Equation (2.1) and Equation (2.2), A is state matrix with assumed dimension $n_1 \times n_1$, B is input matrix with assumed matrix $n_1 \times m$ and C is output matrix with assumed dimension $q \times n_1$, respectively.

Note that from Equation (2.1), the following difference equation is given:

$$x(k) = Ax(k-1) + Bu(k-1) \tag{2.3}$$

The difference of the state variable and control variable are:

$$\Delta x(k+1) = x(k+1) - x(k) \tag{2.4}$$

$$\Delta x(k) = x(k) - x(k-1) \tag{2.5}$$

$$\Delta u(k) = u(k) - u(k-1) \tag{2.6}$$

Taking a difference operation on both sides of Equation (2.1), obtain

$$x(k+1) - x(k) = A(x(k) - x(k-1)) + B(u(k) - u(k-1)) \tag{2.7}$$

Therefore

$$\Delta x(k+1) = A\Delta x(k) + B\Delta u(k) \tag{2.8}$$

In order to relate the output $y(k)$ to the state variable $\Delta x(k)$, yields that

$$\begin{aligned} \Delta y(k+1) &= y(k+1) - y(k) \\ &= Cx(k+1) - Cx(k) \\ &= C\Delta x(k+1) \\ &= CA\Delta x(k) + CB\Delta u(k) \end{aligned} \tag{2.9}$$

$$\tag{2.10}$$

Then

$$y(k+1) = y(k) + CA\Delta x(k) + CB\Delta u(k) \tag{2.11}$$

Putting together Equation (2.8) with Equation (2.11) leads to the following state-space model:

$$\overbrace{\begin{bmatrix} \Delta x(k+1) \\ y(k+1) \end{bmatrix}}^{\bar{x}(k+1)} = \overbrace{\begin{bmatrix} A & O^T \\ CA & I_{q\times q} \end{bmatrix}}^{\bar{A}} \overbrace{\begin{bmatrix} \Delta x(k) \\ y(k) \end{bmatrix}}^{\bar{x}(k)} + \overbrace{\begin{bmatrix} B \\ CB \end{bmatrix}}^{\bar{B}} \Delta u(k) \tag{2.12}$$

$$y(k) = \overbrace{\begin{bmatrix} O & I_{q\times q} \end{bmatrix}}^{\bar{C}} \begin{bmatrix} \Delta x(k) \\ y(k) \end{bmatrix} \tag{2.13}$$

where $I_{q\times q}$ is the identity matrix with dimension $q \times q$, and q is the number of outputs; and o_m is a $q \times n_1$ zero matrix. $\bar{x}(k+1)$ and $\bar{x}(k)$ are the new states. The triplet $(\bar{A}, \bar{B}, \bar{C})$ is called the augmented model, which is used in the design of predictive control [5]. The augmented model contains integrators which serve to eliminate steady state error. In next subsection, these matrices are derived for the adaptive cruise control (ACC) model.

2.2.2 Vehicle Following Model

Adaptive cruise control models described dynamic relationships between vehicles including relative position, relative velocity and acceleration. Longitudinal control ensures equal speeds of leader and follower vehicles as well as stable distances between them. The safety distance is a function of the dynamics of the vehicle. The model below is typical to describe the relative dynamic of the following and leading vehicles [11].

$$\begin{bmatrix} x_r(k+1) \\ v_r(k+1) \end{bmatrix} = \begin{bmatrix} 1 & T_s \\ 0 & 1 \end{bmatrix} \begin{bmatrix} x_r(k) \\ v_r(k) \end{bmatrix} + \begin{bmatrix} -\frac{1}{2}T_s^2 \\ -T_s \end{bmatrix} u(k) \tag{2.14}$$

where $u(k)$ is the relative acceleration between the following vehicle and leading vehicle, the distance is denoted as $x_r(k)$ and $v_r(k)$ represents the relative velocity between the two vehicles. Note that this model is simply a kinematic relationship between the relative accelerations of the vehicles and the resulting speed and position. For the purpose of this thesis it is assumed that a vehicle acceleration can be commanded directly (i.e the longitudinal vehicle dynamics are ignored). It is important to remember that T_s is equal to $0.001s$, which is the operating frequency of MicroAutoBox [7]. The output variables are the distance and the relative velocity, where

$$y(k) = \begin{bmatrix} 1 & 0 \\ 0 & 1 \end{bmatrix} \begin{bmatrix} x_r(k) \\ v_r(k) \end{bmatrix} \tag{2.15}$$

The augmented model for the vehicle following model.

$$\begin{bmatrix} \Delta x_r(k+1) \\ \Delta v_r(k+1) \\ x_r(k+1) \\ v_r(k+1) \end{bmatrix} = \begin{bmatrix} 1 & T_s & 0 & 0 \\ 0 & 1 & 0 & 0 \\ 1 & T_s & 1 & 0 \\ 0 & 1 & 0 & 1 \end{bmatrix} \begin{bmatrix} \Delta x_r(k) \\ \Delta v_r(k) \\ x_r(k) \\ v_r(k) \end{bmatrix} + \begin{bmatrix} -\frac{1}{2}T_s^2 \\ -T_s \\ -\frac{1}{2}T_s^2 \\ -T_s \end{bmatrix} \Delta u(k) \tag{2.16}$$

$$y(k) = \begin{bmatrix} 0 & 0 & 1 & 0 \\ 0 & 0 & 0 & 1 \end{bmatrix} \begin{bmatrix} \Delta x_r(k) \\ \Delta v_r(k) \\ x_r(k) \\ v_r(k) \end{bmatrix} \tag{2.17}$$

where

$$\Delta x_r(k) = x_r(k) - x_r(k-1) \tag{2.18}$$

$$\Delta v_r(k) = v_r(k) - v_r(k-1) \tag{2.19}$$

$$\Delta u(k) = u(k) - u(k-1) \tag{2.20}$$

Now there are four states in the augmented model, the deviation between the current distance and the previous distance, the deviation between current relative speed between the previous relative speed, the actual distance and relative speed. There are integrators with the augmented model. In next chapter, the longitudinal controller is incorporated into the MPC formulation.

2.3 Conclusion

In this chapter, the concept of vehicle automated following was discussed. Following this, the development of vehicle following model which describes the longitudinal relative dynamics was presented. Augmented model, which adds the error states to the actual states, was specific designed for MPC. The benefit is that there is always at least one integrator in the model, which serve to eliminate the steady state error. Augmented model was designed based on the vehicle following model, which will be used in the design of LMPC controller.

Chapter 3

Controller Design based on Model Predictive Control

3.1 Introduction

This chapter begins with a thorough description of the conventional model predictive control (CMPC) and Laguerre functions based model predictive control (LMPC). Compared to the CMPC, LMPC is available to be tuned by selecting decay factor of Laguerre functions. The constraints on the acceleration and the difference of acceleration are determined based on the experimental results of TORC speed controller. With the constraints, the performance of the closed-loop system are compared to validate the performance of different decay factors. The formulation of MPC below is referenced primarily from [5].

3.2 Basic Idea of Model Predictive Control

Assuming that at current time k_i, $k_i > 0$, the state $x(k_i)$ provides the current plant information using the state equations

$$x(k_i + j + 1 \mid k_i) = Ax(k_i + j \mid k_i) + B\Delta u(k_i + j) \tag{3.1}$$

$$y(k_i + j \mid k_i) = Cx(k_i + j \mid k_i) \tag{3.2}$$

With given information $x(k_i)$, from the Equation (3.1) and Equation (3.2), the future states and future outputs can be predicted from:

$$x(k_i + 1 \mid k_i), \quad x(k_i + 2 \mid k_i) \quad ... \quad x(k_i + k \mid k_i) \quad ... \quad x(k_i + N_P \mid k_i) \tag{3.3}$$

$$y(k_i + 1 \mid k_i), \quad y(k_i + 2 \mid k_i) \quad ... \quad y(k_i + k \mid k_i) \quad ... \quad y(k_i + N_P \mid k_i) \tag{3.4}$$

where the predicted states and output variables are denoted as $x(k_i+k \mid k_i)$ and $y(k_i+k \mid k_i)$ respectively at time $k_i + k$, and N_P is defined as the prediction horizon. Assuming that the future control trajectory are denoted as

$$\Delta u(k_i), \quad \Delta u(k_i+1) \quad ... \quad \Delta u(k_i+k \mid k_i) \quad ... \quad \Delta u(k_i+N_c-1) \tag{3.5}$$

where N_c is defined as the control horizon. Typically, the control horizon N_c should be chosen to be less than (or equal to) the prediction horizon N_P. The predicted state variables can be formulated in terms of current state variables $x(k_i)$ and future control movement $\Delta u(k_i + k \mid k_i)$as below:

$$\begin{aligned}
x(k_i+1 \mid k_i) &= Ax(k_i) + B\Delta u(k_i) \qquad (3.6)\\
x(k_i+2 \mid k_i) &= Ax(k_i+1) + B\Delta u(k_i+1)\\
&= A^2x(k_i) + AB\Delta u(k_i) + B\Delta u(k_i+1)\\
&...\\
x(k_i+N_P \mid k_i) &= A^{N_p}x(k_i) + A^{N_p-1}B\Delta u(k_i)\\
&+ A^{N_p-2}B\Delta u(k_i+1) + ... + A^{N_p-N_c}B\Delta u(k_i+N_c-1)
\end{aligned}$$

The predicted output variables are denoted by:

$$\begin{aligned}
y(k_i+1 \mid k_i) &= CAx(k_i) + CB\Delta u(k_i) \qquad (3.7)\\
y(k_i+2 \mid k_i) &= CAx(k_i) + CB\Delta u(k_i+1)\\
&= CA^2x(k_i) + CAB\Delta u(k_i) + CB\Delta u(k_i+1)\\
&...\\
y(k_i+N_P \mid k_i) &= CA^{N_p}x(k_i+1) + CA^{N_p-1}B\Delta u(k_i)\\
&+ CA^{N_p-2}B\Delta u(k_i+1) + ... + CA^{N_p-N_c}B\Delta u(k_i+N_c-1)
\end{aligned}$$

The predicted states and output states are expressed as the functions of the current states and the future control movements. The next step is to minimize the cost function to find the optimal control horizon. Assuming that at time k_i, R_s is the set-point matrix defined as:

$$R_s^T = \overbrace{[1 \;\; 1 \;\; ... \;\; 1]}^{N_p} r(k_i) \tag{3.8}$$

where $r(k_i)$ is the set-point signal for the output $y(k_i)$ at time k_i. The cost function is defined as

$$J = (R_s - Y)^T (R_s - Y) + \Delta U^T R \Delta U \tag{3.9}$$

where

$$Y = [y(k_i + 1 \mid k_i) \;\; y(k_i + 2 \mid k_i) \;\; y(k_i + 3 \mid k_i) \;\; ... \;\; y(k_i + N_p \mid k_i)]^T \tag{3.10}$$

$$\Delta U = [\Delta u(k_i) \;\; \Delta u(k_i + 1) \;\; ... \;\; \Delta u(k_i + k) \;\; ... \;\; \Delta u(k_i + N_c - 1)]^T \tag{3.11}$$

and R is a diagonal matrix. The objective of the predictive control system is to bring the predicted outputs as close as possible to the set-point signal. The control horizon is achieved by minimizing the error function between the set-point and the predicted outputs. After the control horizon is obtained, the first item of the horizon ($\Delta u(k_i + 1)$) is implemented in control system. Then another control sequence $\Delta U(k_{i+1})$ is calculated at the next sampling instant k_{i+1}.

3.3 Optimization of Incremental Control using Laguerre Functions

3.3.1 Discrete-time Laguerre Networks

The core technique in the design of discrete MPC is based on optimizing the future control trajectory, that is the difference of the control signal ($\Delta u(k)$). By assuming a finite control horizon N_c, the difference of the control signal is expressed by $\Delta u(k)$ for $k = 1, 2, ..., N_c$.

The Laguerre functions are introduced into the design to generalize the design procedure [9]. These functions will help reformulate the predictive control problem and simplify the solutions. The control system is available to tune by different decay factors of Laguerre functions. At time k_i, the control variable is regarded as the impulse response of a stable system. Thus, a set of Laguerre functions, $l_1(k), l_2(k), ..., l_N(k)$ are used to capture this dynamic response with a set of Laguerre coefficients that is determined iteratively from the design process. More precisely, at arbitrary future sampling instant k,

$$\Delta u(k_i + k) = \sum_{j=1}^{N} c_j l_j(k); \tag{3.12}$$

with k_i being the initial time and k being the future sampling instant; N is the number of terms used in the expansion and $c_j, j = 1, 2, ..., N$, are the coefficients. $l_j(k)$ are the set of discrete Laguerre functions. From the definition of Laguerre functions, the z-transform representations are,

$$\Gamma_N(z, a) = \frac{\sqrt{1 - a^2}}{1 - az^{-1}} (\frac{z^{-1} - a}{1 - az^{-1}})^{N-1} \tag{3.13}$$

where a is the pole of the discrete-time Laguerre network and N is the number of network terms respectively. The Laguerre network is illustrated in Figure 3.1.

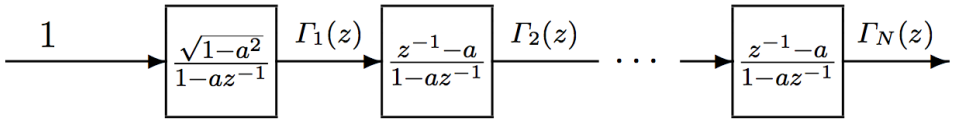

Figure 3.1: Discrete Laguerre network

Note that a is selected by the user [5], [9]. The stability of the network can be guaranteed when $0 < a < 1$. The approximation to the impulse response depends on the selection of a and N. Furthermore, from Equation (3.13), the set of difference equations that the discrete Laguerre functions satisfy

$$L(k + 1) = \Omega L(k) \tag{3.14}$$

where

$$\Omega = \begin{bmatrix} a & 0 & ... & 0 \\ 1-a^2 & a & ... & 0 \\ a(1-a^2) & 1-a^2 & ... & 0 \\ a^2(1-a^2) & a(1-a^2) & ... & 0 \\ ... & ... & ... & ... \\ a^{N-2}(1-a^2) & a^{N-3}(1-a^2) & ... & a \end{bmatrix} \tag{3.15}$$

$$L(k) = [l_1(k) \;\; l_2(k) \;\; \dots \;\; l_N(k)]^T \tag{3.16}$$

with initial condition

$$L(0) = \sqrt{1-a^2}[1 \;\; a \;\; a^2 \;\; a^3 \;\; ... \;\; a^{N-1}]^T \tag{3.17}$$

Another important property of the Laguerre functions is the orthonormal property, which can be expressed by:

$$\begin{cases} \sum_{k=0}^{N_p} l_i(k) l_j(k) = 0, if \;\; i \neq j \\ \sum_{k=0}^{N_p} l_i(k) l_j(k) = 1, if \;\; i = j \end{cases} \tag{3.18}$$

This property is used for finding the minimum of the cost function later. The impulse response of the system are approximated by selecting different values of a and N. Here, a is selected equal to 0.3, 0.6, 0.9 and N is set to be 10, 20 and 50. The results are shown in Figure 3.2 - 3.4 for the various values. There are 50 parameters required to capture the response when $a = 0$. Increasing a requires less parameters to capture the response. For example, 50 parameters are needed when a is equal to 0.3, 20 parameters are needed when a equal to 0.6, and only 10 parameters are needed when a is equal to 0.9.

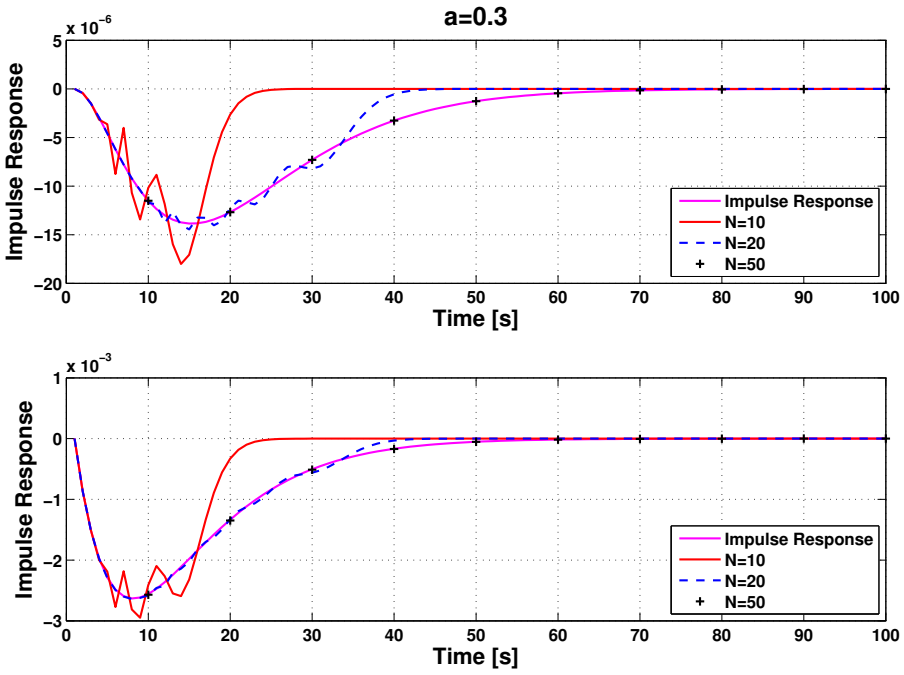

Figure 3.2: Approximation to the Impulse Response ($a = 0.3$)

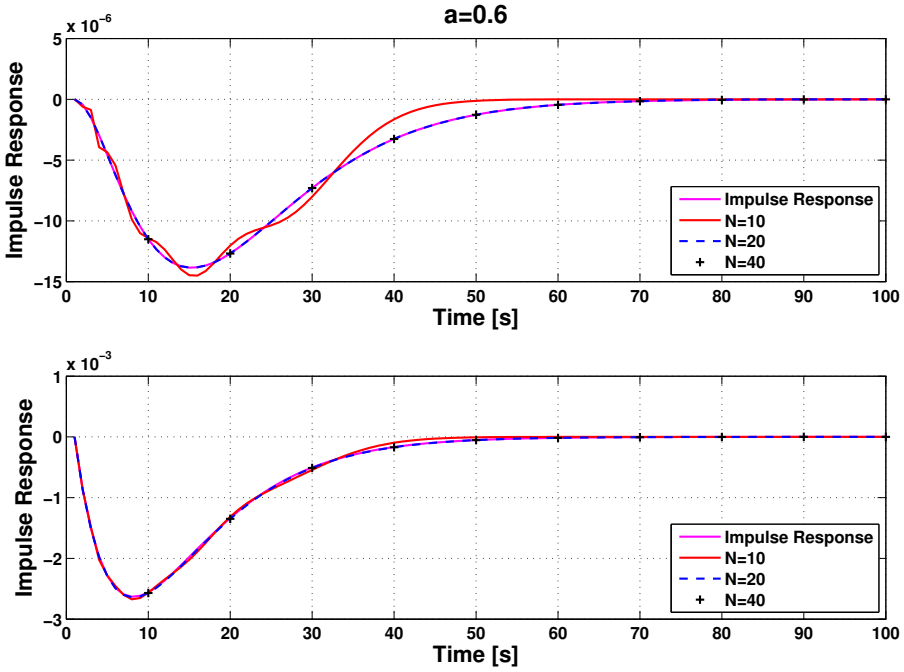

Figure 3.3: Approximation to the Impulse Response ($a = 0.6$)

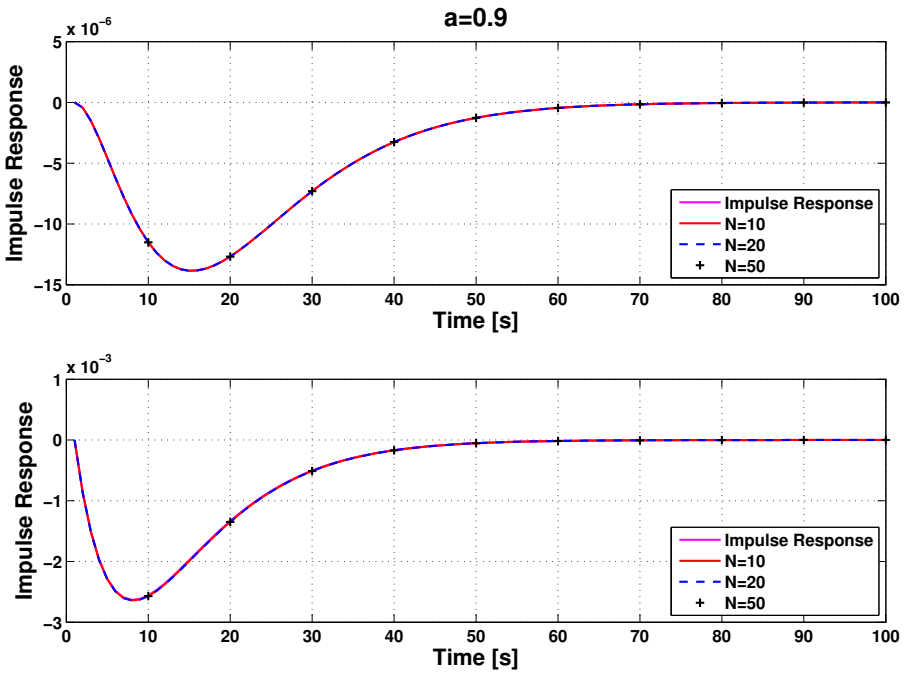

Figure 3.4: Approximation to the Impulse Response ($a = 0.9$)

3.3.2 Minimization of Cost Function

When Laguerre functions are applied to the control variables, Equation (3.12) can be re-written in a vector form:

$$\Delta u(k_i + k) = L(k)^T \eta = \begin{bmatrix} l_1(k) & l_2(k) & \dots & l_N(k) \end{bmatrix} \begin{bmatrix} c_1 \\ c_2 \\ \dots \\ c_N \end{bmatrix} \tag{3.19}$$

Hence, the future control trajectory is populated as:

$$\Delta U = \begin{bmatrix} \Delta u(k_i) \\ \Delta u(k_i+1) \\ ... \\ \Delta u(k_i+k) \\ ... \\ \Delta u(k_i+N_c-1) \end{bmatrix} = \begin{bmatrix} l_1(0) & l_2(0) & ... & l_N(0) \\ l_1(1) & l_2(1) & ... & l_N(1) \\ & & ... & \\ l_1(k) & l_2(k) & ... & l_N(k) \\ & & ... & \\ l_1(N_c-1) & l_2(N_c-1) & ... & l_N(N_c-1) \end{bmatrix} \begin{bmatrix} c_1 \\ c_2 \\ ... \\ c_k \\ ... \\ c_N \end{bmatrix} \tag{3.20}$$

where N is the number of Laguerre networks and N_c is length of the control horizon. Compared to the Equation (3.11), the control variables are expressed by Laguerre functions. Here, the special case is investigated when $a = 0$ such that Ω becomes

$$\Omega = \begin{bmatrix} 0 & 0 & 0 & ... & 0 & 0 \\ 1 & 0 & 0 & ... & 0 & 0 \\ 0 & 1 & 0 & ... & 0 & 0 \\ ... & ... & ... & ... & ... & ... \\ 0 & ... & ... & 0 & 1 & 0 \end{bmatrix} \tag{3.21}$$

$$L(0)^T = [1 \;\; 0 \;\; 0 \;\; 0 \;\; ... \;\; 0] \tag{3.22}$$

Then the control trajectory becomes the "vector" of Laguerre coefficients, $c_j ... c_{N_c}$ as represented by

$$\Delta U = [c_1 \;\; c_2 \;\; c_3 \;\; ... \;\; c_{N_c}]^T \tag{3.23}$$

which is equivalent to Equation (3.11), the Laguerre coefficients take the place of the control inputs at each future time instant accordingly. When $a = 0$, the MPC design using Laguerre functions is equivalent to the CMPC.

Since the control trajectory is expressed using Laguerre functions, given the augmented model (A,B,C) with ΔU as the input signal with the initial state variable information $x(k_i)$,

the prediction of the future state variable, $x(k_i + k \mid k_i)$ at sampling instant $k_i + k$, becomes

$$x(k_i + k \mid k_i) = A^k x(k_i) + \sum_{i=0}^{k-1} A^{k-i-1} BL(i)^T \eta \tag{3.24}$$

where $\Delta u(k_i + k)$ is replaced by $L(k)^T \eta$. Similarly, the prediction for the plant output at future sampling instant $k_i + k$ is

$$y(k_i + k \mid k_i) = CA^k x(k_i) + \sum_{i=0}^{k-1} CA^{k-i-1} BL(i)^T \eta \tag{3.25}$$

With this formulation, both predictions of states and outputs are expressed in terms of the coefficient vector η, and the task becomes finding the coefficient vector η which can minimize the cost function.

Recall the cost function defined by Equation (3.9), noting that Y ad ΔU are in the vector form, it is equivalent to

$$J = \sum_{k=1}^{N_p} (r(k_i) - y(k_i + m) \mid k_i))^T Q (r(k_i) - y(k_i + m) \mid k_i)) + \sum_{m=0}^{N_p} \Delta u(k_i + m)^T R \Delta u(k_i + m) \tag{3.26}$$

Here, the cost function is re-formulated with a link to discrete-time linear quadratic regulator (DLQR) [30], where

$$J = \sum_{k=1}^{N_p} x(k_i + k \mid k_i)^T Q x(k_i + k \mid k_i) + \sum_{k=0}^{N_p} \Delta u(k_i + k)^T R \Delta u(k_i + k) \tag{3.27}$$

with the weighting matrices $Q \geq 0$ and $R > 0$. In particular, Q has the dimension equal to the number of state variables and R has the dimension equal to dimension η. The reason for this re-formulation is to connect the discrete-time MPC with the DLQR system so that the numerous classical results in DLQR will lend themselves to the analysis, tuning and design of discrete-time MPC. The cost function for minimization of output errors defined by Equation (3.9) is identical to the cost function defined by Equation (3.27) [5]. Replacing $\Delta u(k_i + k)$

by Equation (3.19), and combining with the orthonormal property represented by Equation (3.18), the cost function Equation (3.27) can be simplified as:

$$J = \sum_{k=1}^{N_p} x(k_i + k \mid k_i)^T Q x(k_i + k \mid k_i) + \eta^T R \eta \tag{3.28}$$

Using the Equation (3.24) and defining the matrix $\phi(k)^T = \sum_{i=0}^{k-1} A^{k-i-1} B L(i)^T$, results in the function becoming

$$\begin{aligned} J &= \eta^T (\sum_{k=1}^{N_p} \phi(k) Q \phi(k)^T + R)\eta \\ &+ 2\eta^T (\sum_{k=1}^{N_p} \phi(k) Q A^k) x(k_i) + \sum_{k=1}^{N_p} x(k_i)^T (A^T)^k Q A^k x(k_i) \end{aligned} \tag{3.29}$$

To find the minimum of Equation (3.29), without constraints, the derivative of the cost function is,

$$\frac{\partial J}{\partial \eta} = 2(\sum_{k=1}^{N_p} \phi(k) Q \phi(k)^T + R)\eta) + 2(\sum_{k=1}^{N_p} \phi(k) Q A^k) x(k_i) \tag{3.30}$$

Assuming that$(\sum_{k=1}^{N_p} \phi(k) Q \phi(k)^T + R)^{-1}$ exists, when $\frac{\partial J}{\partial \eta} = 0$, the optimal solution of the parameter vector η [5]is

$$\eta = -(\sum_{k=1}^{N_p} \phi(k) Q \phi(k)^T + R)^{-1} (\sum_{k=1}^{N_p} \phi(k) Q A^k) x(k_i) \tag{3.31}$$

For simplicity of the expression, the components of η are defined as:

$$\Omega = \sum_{k=1}^{N_p} \phi(k) Q \phi(k)^T + R \tag{3.32}$$

$$\Psi = \sum_{k=1}^{N_p} \phi(k) Q A^k \tag{3.33}$$

leading to

$$\eta = -\Omega^{-1}\Psi x(k_i) \tag{3.34}$$

where $x(k_i)$ is the state at sampling instant k_i. The optimal parameter η is found which can minimize the cost function. After obtaining the optimal parameter vector η, the control trajectory can be computed when k is set to be 0.

$$\begin{aligned} U &= \Omega \times \eta \qquad (3.35) \\ &= -\Psi x(k_i) \end{aligned}$$

$$(3.36)$$

The first term of U is used as the input of the system and the receding horizon control law is realized as

$$\Delta u(k_i) = L(0)^T \eta \tag{3.37}$$

Also, the control $\Delta u(k_i)$ can be written

$$\Delta u(k_i) = -L(0)^T \Omega^{-1} \Psi x(k_i) \tag{3.38}$$

Now the control variable computed at each sampling instant is a function of the current measurements of the states. In this work, the states are the deviation between the current distance and the previous distance, the deviation between current relative speed between the previous relative speed, the actual distance and relative speed defined by Equation (2.16).

3.4 Constraints

3.4.1 Test of TORC Speed Controller

The acceleration capability of the real vehicle is limited in practice. The constraints on the control variables and the difference of the control variables ensure that the desired acceleration is possible to implement in the experimental vehicle. The constraints on the inputs are expressed as u_{min} and u_{max} and the constraints on the difference of the control variables are denoted by Δu_{min} and Δu_{max}. Note u represents the acceleration and Δu is the difference of the acceleration in this work. Suppose that at sample time k_i, the previous control signal is $u(k_i - 1)$. The system is subject to constraints of the form

$$\begin{cases} u_{min} \leq u(k_i) \leq u_{max} \\ \Delta u_{min} \leq \Delta u(k_i) \leq \Delta u_{max} \end{cases} \tag{3.39}$$

The difference of desired acceleration (Δu) is computed depending on three different cases:

$$\Delta u(k_i) = \begin{cases} u_{min} - u(k_i - 1), if \;\; u(k_i) \leq u_{min} \\ L(0)^T \eta, if \;\; u_{min} < u(k_i) < u_{max} \\ u_{max} - u(k_i - 1), if \;\; u(k_i) \geq u_{max} \end{cases} \tag{3.40}$$

In this work, the acceleration limits used as the global limits are determined based on the acceleration ability of the test vehicles. The TORC speed controller discussed in Chapter 4 is used as the lower controller. In order to acquire the acceleration ability of the test vehicles, several trials were carried out to evaluate the performance of the TORC speed controller. The TORC controller can regulate the speed of the vehicle automatically depending on the speed commands, therefore speed commands were sent directly to the TORC controller. The inner control method of the TORC speed controller is a PID control, and the coefficients of a PID are 0.1, 0.01 and 0.001. The test procedure was:

- First, turn on the ACC function of the vehicle by speeding up the vehicle more than 25km/h. Then set the control mode to mode 1 through the ControlDesk interface.
- When the control mode is set to be mode 1, the speed of the vehicle will be controlled by desired speed command set via the ControlDesk interface.
- The desired speed commands are set by hand through the ControlDesk. The desired speed commands were 6.9444 m/s at 0s, 11.111m/s at 5s, 5.5666 m/s at 9s, 4.1667 m/s at 12s and 8.333 m/s at 15s. After 19s, the TORC speed controller is disabled and the vehicle is taken over by the driver. The time and the speed value were selected randomly.

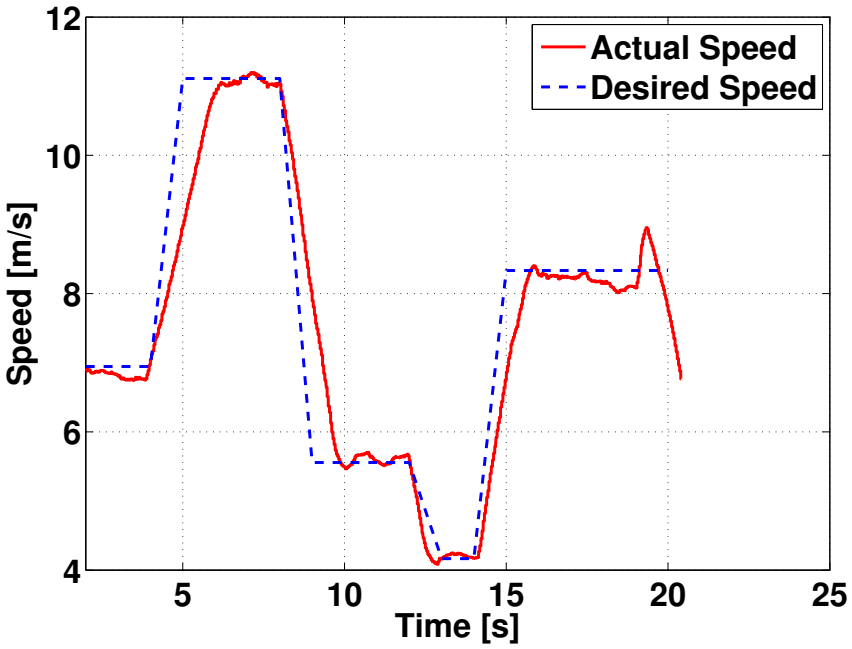

Figure 3.5: Step Change in Set Speed of the TORC Speed Controller

The experimental results are shown in Figure 3.5, where it is shown that the actual speed of the vehicle can track the desired speed fairly well. Also, the accelerating ability is evaluated from the test results, where u_{max} and u_{min} are $2m/s^2$ and $-3m/s^2$ when the

coefficients of PID are 0.1, 0.01, 0.001. The acceleration limits, u_{max} and u_{min}, are reasonably set to be

$$u_{max} = 1.5m/s^2 \tag{3.41}$$

$$u_{min} = -1.5m/s^2 \tag{3.42}$$

$-1.5m/s^2$ and $-1.5m/s^2$ in the tests, which are smaller than the vehicle acceleration capability. The constraints of Δu are

$$\Delta u_{max} = 1.5m/s^2 \tag{3.43}$$

$$\Delta u_{min} = -1.5m/s^2 \tag{3.44}$$

The smaller acceleration or deceleration should be achievable. The other considerations for the acceleration limits are the length of test field and ride comfort.

3.5 Use of Laguerre Functions as Tuning Parameters

The simulation results, obtained with the numerical values of the model given in Chapter 2, and the terminal cost function and constraints calculated in Chapter 3, are presented in this section. The LMPC is considered successful if the following vehicle can follow the target vehicle with a desired distance and the same speed, with the desired acceleration, and the difference of the desired acceleration limits imposed. The simulations are executed in Matlab. When Laguerre functions are used to describe the control horizon, different a and N values affect the closed-loop performance of the LMPC system. This is particularly useful when the CMPC can not provide a satisfactory closed-loop performance. Laguerre functions are a set of exponential functions with a decay factor a when $0 < a < 1$. The incremental control signal $\Delta u(k_i + k)$ is forced to decay exponentially as k increases [8]. Different decay factors affect the closed-loop performance, which is shown through simulations with Matlab. In

order to ensure N is large enough to capture the response for all a, the parameter N is set to a value of 50. Because the sampling time is 0.001s, a large number of predictions is needed to ensure the stability of the closed-loop system. Therefore, the number of prediction used is $N_p = 1900$. The pole location a is chosen as $a = 0, a = 0.1, a = 0.5, a = 0.9$. The acceleration limits are $-1.5m/s^2$ and $1.5m/s^2$ and the constraints on the difference of the acceleration are $-1.5m/s^2$ and $1.5m/s^2$. The state weighting matrix (Q) and input weighting matrix (R) are

$$Q = \begin{bmatrix} 0 & 0 & 0 & 0 \\ 0 & 0 & 0 & 0 \\ 0 & 0 & 10 & 0 \\ 0 & 0 & 0 & 1 \end{bmatrix} \tag{3.45}$$

$$R = 1 \tag{3.46}$$

To test the effect of different values of a, simulations were run with the constraints. Table 3.1 and Table 3.2 show the eigenvalues of the closed-loop system for the cases for the various a values.

Table 3.1: Discrete Eigenvalues of Closed-loop System of different decay factors (a)

a	Eigenvalues of Closed-loop System
a=0	[0.9606 + 0.0288i 0.9606 - 0.0288i 0.9928 1]
a=0.5	[0.9776 + 0.0220i 0.9776 - 0.0220i 0.9965 1]
a=0.9	[0.9777 + 0.0219i 0.9777 - 0.0219i 0.9968 1]

Table 3.2: Feedback gain of Closed-loop System of different decay factors (a)

a	Feedback Gain
a=0	[-2794.7 -79.5 -4.3 0.3]
a=0.5	[-1037.3 -47.6 -3.5 -1]
a=0.9	[-1107.8 -47.2 -3.1 0]

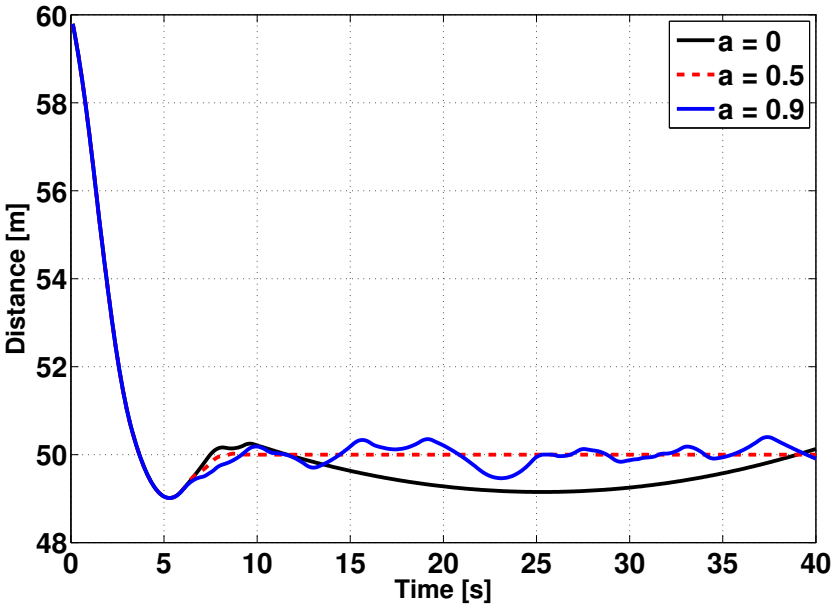

Figure 3.6: Distance between Leader and Follower

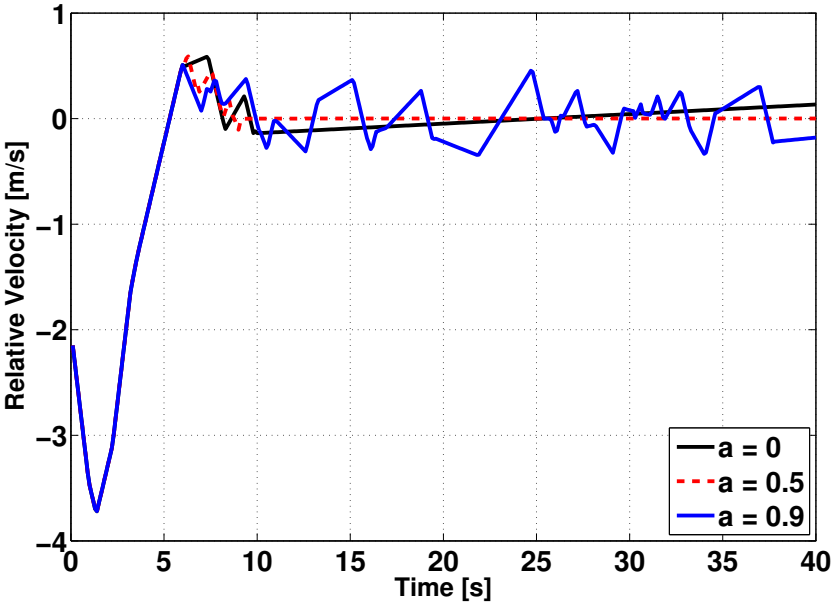

Figure 3.7: Relative Speed between Leader and Follower

The effect of a on the eigenvalues of the closed-loop system is shown in Table 3.1. Figure 3.6 shows the simulated distance with the initial value of 60 m, Figure 3.7 represents the simulated relative speed with the initial value of $-2\,m/s$. The effect of the decay factor can be seen in these plots. When $a = 0$, the LMPC becomes the CMPC and the desired distance and the desired relative speed can not be achieved with the constraints of control variable. The distance is brought to 50 meters and the relative speed is brought to 0 when a is 0.5. Between the three parameters $a = 0.5$ was determined to be the best. The performance of the closed-loop system is desirable. The LMPC proved to be very sensitive to the different values of a. Note that when a is increased to 0.9, the system becomes unstable again. The parameter a affects the closed-loop system performance, but there is no specific relationship between the value of a and the performance. In addition to using the weighting matrices Q and R to tune the system, it is feasible to use a as another tuning parameter. The LMPC is more flexible compared to the conventional solution methodology and presents another way to tune the control system. In the simulation, controller works well with the ideal case, which is that the desired acceleration can be acquired immediately.

3.6 Conclusion

The basic idea of MPC was presented. Future states are predicted and the optimal solution is achieved by minimizing the errors between the set-points and the predicted outputs. Compared to the CMPC, the control variables are expressed using Laguerre functions. The cost function is simplified and it is easier to find the optimal solution due to of the orthonormal property of Laguerre functions. Additionally, the Laguerre functions are a set of exponential functions with a decay factor such that the incremental control signal is also forced to decay exponentially when it is expressed by Laguerre functions. In the cost function, more emphasis is placed on the control trajectory at the current time and less emphasis on those at future times as the sampling instant increases. The closed-loop performance is

susceptible to the different decay factors of the Laguerre functions. With a given cost function, the LMPC provides another method to tune the performance of the MPC system. Constraints are determined based on the experimental data of TORC speed controller. Simulation results were presented to illustrate the closed-loop performance of different Laguerre coefficients.

Chapter 4

Experimental Validation

4.1 Introduction

In this chapter, an experimental platform consisting of a PinPoint navigation system, Dedicated Short Range Communications (DSRC), Embedded PC, and MicroAutobox are introduced. The PinPoint is a continuous positioning system. DSRC is used as V2V communication. The embedded PC is the communication bridge between the PinPoint, DSRC, and MicroAutobox. The TORC Automative Interface Module is a user defined speed controller which can regulate the speed of vehicle through the CAN Bus. Experimental data is collected to evaluate the performance of TORC controller and LMPC controller. Analysis of the experimental data is given to explain the overshoot of distance and errors of the relative speed. Solutions are given and evaluated by simulation to improve the performance of future experiments.

4.2 System Architecture

As shown in Figure 4.1 and Figure 4.2, the system includes a PinPoint (navigation system), DSRC (communication radio), Embedded PC, MicroAutobox and TORC controller. More information about the hardware is presented below. Navigation and localization information of the host vehicle are achieved from PinPoint and the information from leading vehicle is received from DSRC. All the messages are sent to the Embedded PC, which is a communication bridge between the PinPoint, DSRC, and the MicroAutobox. The vehicle information from the Embedded PC and CAN Bus are the inputs of the control algorithm running in the MicroAutobox. The desired speed generated from the control algorithm is

sent to the TORC speed controller, which is used to regulate the following vehicle speed.The test vehicles are 2014 Cadillac SRX as shown in Figure 4.3. Each vehicle is equipped with the PinPoint, DSRC, MicroAutoBox, Embedded PC and other support devices such as power distribution system. Also, the vehicle speed, the throttle position and the other information of the vehicle can be obtained via a controller area network (CAN) bus. This information are potentially useful for future work such as automated lane change. In this work, velocity from the CAN Bus is used for calculating the relative velocity.

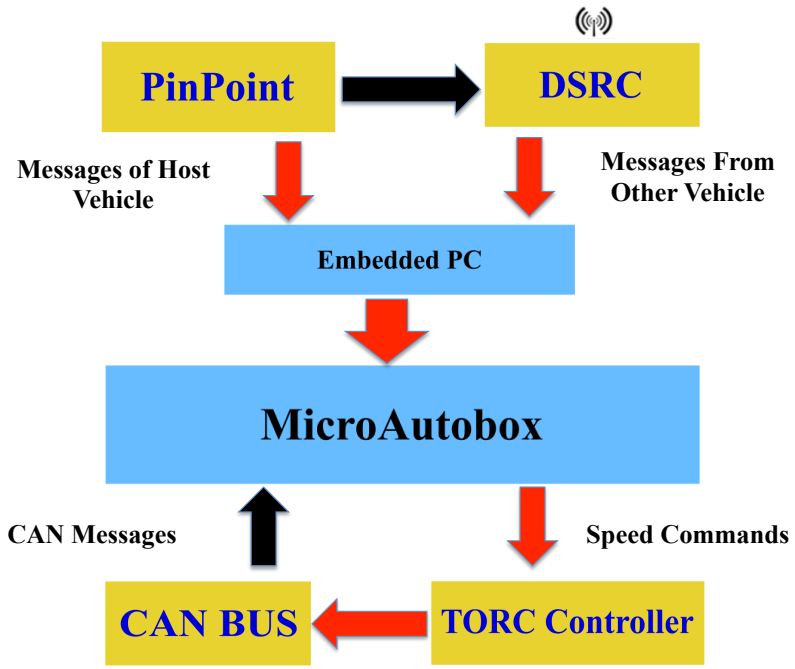

Figure 4.1: System Infrastructure

4.3 Hardwares Descriptions

4.3.1 PinPoint Localization Module

The PinPoint localization system shown in Figure 4.4 is a continuous positioning system for ground vehicles [10]. It provides multi-sensor fusion of dual-GPS receivers, inertial

Figure 4.2: Experimental setup in the vehicle which includes MicroAutoBox, DSRC and PinPoint

Figure 4.3: Cadillac SRX used for the experimental test

sensors, and wheel speed sensors to provide real time position, orientation, velocity, and time information. Also, PinPoint operates with either a low-cost internal IMU or a high-precision

external IMU and is based on an error-state, multiplicative, extended Kalman filter that estimates the vehicles' position, velocity, and attitude. These estimates are propagated in time by the IMU measurements as the vehicle moves, and the GPS and wheel speed sensors are used to correct the estimates in the measurement update phase of the filter. All outputs are continuously updated regardless of a GPS fix, allowing operation during GPS degradation or complete signal loss. High dynamic measurements of the vehicle are provided to the control system. Positions measured from PinPoint compared to the Google maps are shown in Figure 4.5. In this work, PinPoint is used for the navigation which provide position, velocity and acceleration of the vehicles.

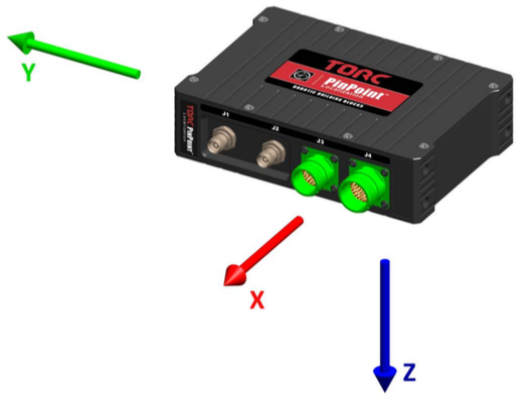

Figure 4.4: PinPoint

4.3.2 DSRC Onboard Equipment (OBE)

Dedicated short-range communications (DSRC) shown in Figure 4.6 are one-way or two-way short-range to medium-range wireless communication channels specifically designed for automotive use and has a unique set of protocols and standards for this purpose. It is a key enabling technology of connected automated vehicle systems. The US Federal Communications Commission allocated 75 megahertz of spectrum in the 5.850-5.925 GHz band for intelligent transportation services [29]. In experiments, the DSRC provides the ability for the SRX vehicles to communicate with the other vehicles reliably.

Figure 4.5: Positions from PinPoint

Figure 4.6: DSRC

4.3.3 MicroAutobox II

The core of the whole system is a MicroAutoBox II (MAB II) shown in Figure 4.7, which is a real-time system for performing fast function prototyping in full pass and bypass scenarios [7]. It operates without user intervention, just like an ECU. MicroAutoBox can

be used for many different rapid control prototyping applications such as: classic control, electric drives control, advanced driver assistance systems and etc. The major advantage is that it provides a means to more rapidly develop and test systems using model-based control design. The MAB II is meant to be used in combination with the dSpace implementation tools and the Simulink modeling environment. With the dSpace implementation tools, a Simulink model can be automatically complied to a real-time application that will run in the MAB II. As shown in Figure 4.1, data from the PinPoint and DSRC is passed to the MAB II through an Ethernet connection.

Figure 4.7: MicroAutoBox [7]

4.3.4 TORC Automotive Interface Module

Maximum and minimum acceleration were determined by the test performance of TORC Speed controller. The TORC Automative Interface Module shown in Figure 4.8 is specifically designed for automated vehicles and is responsible for the speed control. When a speed command is received, the TORC module regulates the speed via a user defined command for this test. The control method is proportional-integral-derivative (PID) controller. Here, the coefficients of PID are set to be 0.1, 0.01,0.001, which are determined based on trial and

error running during the experimental data collection. The TORC controller has two modes: mode 0 represents that it is disabled and mode 1 represents that it is enabled.

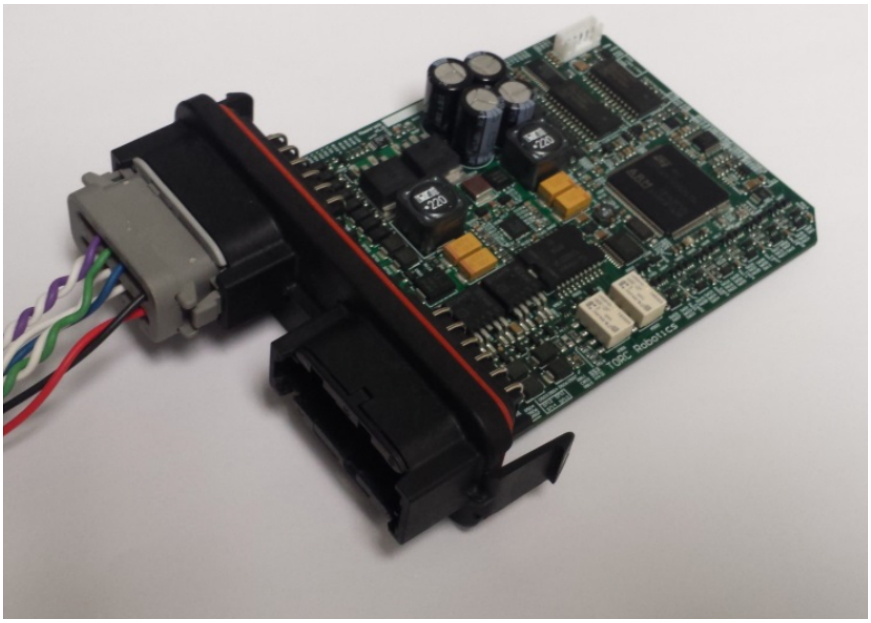

Figure 4.8: TORC Quad CAN ECU Module

4.4 Software Setup

Software associated with the hardware consists of user written programs (c code) and client supplied ControlDesk. The user write programs are required to execute in the test. The information such as position and velocity from PinPoint and DSRC are regarded as the inputs of the MicroAutobox, but the PinPoint and DSRC can not communicate with MicroAutobox directly. The Embedded PC is used as a communication bridge between the PinPoint, DSRC, and MicroAutobox. The programs are responsible for sending the navigation and localization information of PinPoint and DSRC to the Embedded PC. All the information can be displayed on a monitor. The benefit of using MicroAutobox is that the control algorithm can be developed in Simulink. The Simulink model is compiled into a real-time application (*sdf* file), which is running in MicroAutobox. ControlDesk is the interface for the MicroAutobox shown in Figure 4.9. When the *sdf* file is downloaded into

the MicroAutobox, all the variables defined in Simulink model such as desired distance and acceleration limits can be changed and displayed.

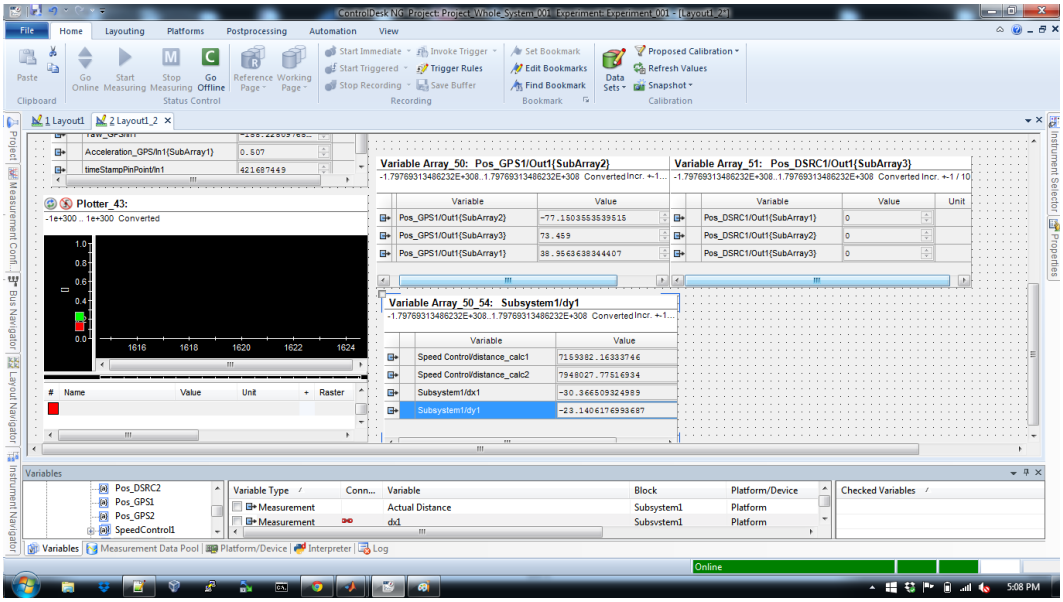

Figure 4.9: User Interface of ControlDesk

4.5 Experimental Results

4.5.1 Test of Vehicle Following Controller

The Laguerre function based model predictive controller presented in this thesis was also evaluated on the two experimental vehicles. Two vehicles as shown in Figure 4.3 are involved in the test. The terrain condition is almost flat with some slightly hilly areas. Both of the vehicles are equipped with V2V communication. In order to implement the designed controller in MicroAutobox, the control algorithm was transferred to Simulink blocks. The Simulink blocks were used for generating the real-time application named *sdf* file.

The Simulink blocks of the controller implementation is shown in Figure 4.10. First, navigation information is collected for processing (Information Acquired). Specifically, the position and speed of leading vehicle are received from DSRC; the position of the following vehicle is received from PinPoint; and the speed and acceleration of following vehicle are

acquired form CAN Bus of the following vehicle. Second, the distance between the two vehicles and relative speed are computed (Calculation). Note, the desired distance (50m) and desired relative speed (0 m/s) have been previously set by the user. After the information is received successfully, the states which are the error between the current relative speed and previous relative speed, the error between the current distance and previous distance, the error between the actual relative speed and desired relative speed (0 m/s) and the error between actual distance and desired distance can be updated. Third, the states multiplied by the feedback gain is the difference of desired acceleration. The sum of the difference of desired acceleration, the acceleration of following vehicle from PinPoint, and the acceleration of leading vehicle from DSRC is the desired acceleration; the desired acceleration multiplied by sampling period plus the current speed is the desired speed. Finally, the desired speed is sent to the TORC speed controller, and the following vehicle speed is regulated by the speed command to maintain the distance and the relative speed.

The MPC controller is executed in real time implementation on a MicroAutoBox platform. The test is performed with a pre-set distance of 50 meters. The test procedure and results are presented below. At the beginning of the test, the following vehicle was driven to 10m/s to enable the ACC function (minimum speed to enable the ACC function is 6.94m/s), so the initial speed of the following vehicle at 0s is about 10m/s. During 0-6.4s, the following speed is set to 5.5 m/s, as shown in Figure 4.12, by sending this speed through TORC speed controller directly. Because the test field is small, these vehicles are tested at low speed. The leading vehicle stops in front of the following vehicle, so the distance is getting closer as shown in Figure 4.11 between 0-6.4s. At about 6.4s, the control switch is set from mode 1 to mode 2, which enables the controller as shown in Figure 4.14. During 6.4-65s, the following vehicle speed is automated controlled by the control algorithm running in the MicroAutoBox without pressing the throttle or brake. Because by the initial speed is larger than the leading speed, in the first phase, the following vehicle is trying to catch up to the

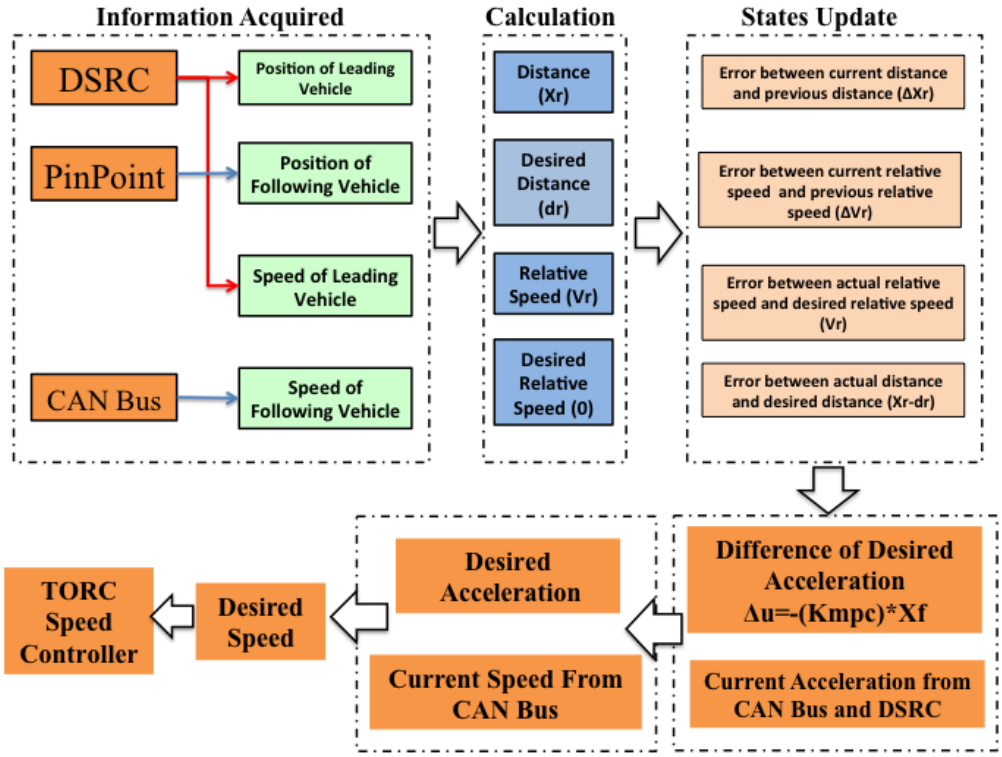

Figure 4.10: Simulink Blocks of Controller Implementation

leading vehicle. When the speeds are almost the same at 20s, the vehicle decelerates to enlarge the distance between the vehicles. At 30s, the distance is brought to 50 meters which is the desired distance, and the relative speed is close to zero, but with some errors. The experimental results show that the controller succeeds in maintaining the desired distance (with some overshoot) and the same speed (with errors) between the leading and following vehicles. After 65s, the following vehicle is decelerated by manually pressing the brake. The ACC function and controller are disabled automatically and without changing the value of control switch. The leading vehicle went further and the experiment was stopped.

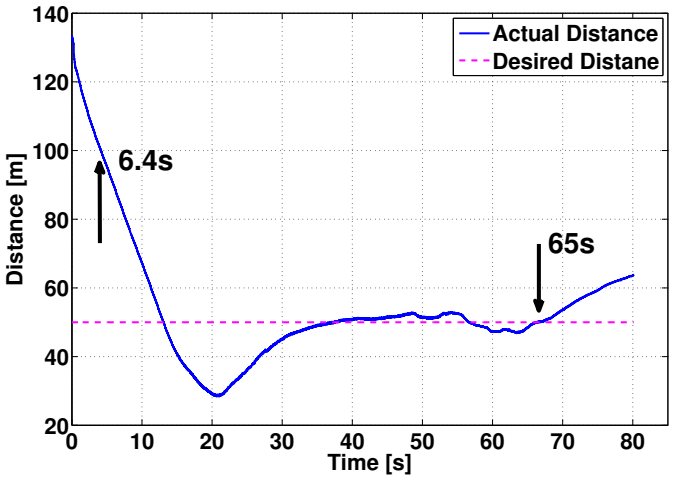

Figure 4.11: Actual Distance

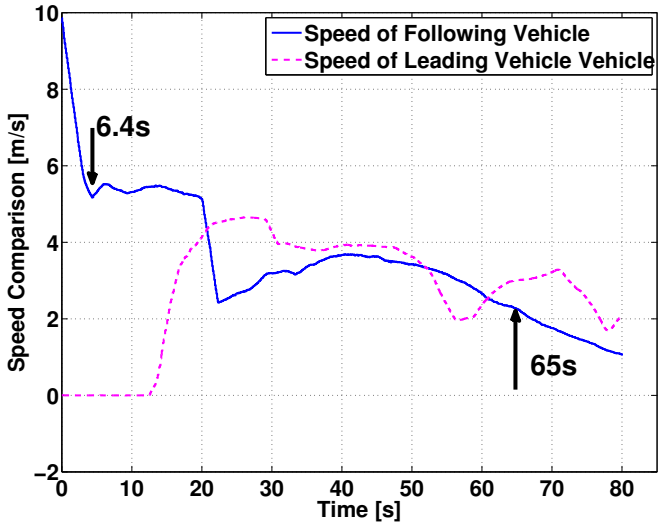

Figure 4.12: Speed Comparison

4.6 Discussion of Experimental Data

4.6.1 Absence of the Acceleration of Leading Vehicle

The vehicles equipped with V2V communication can communicate with each other as discussed previously . Information consists of position, velocity, and acceleration from other vehicles are acquired through V2V communication. In general the control system based on

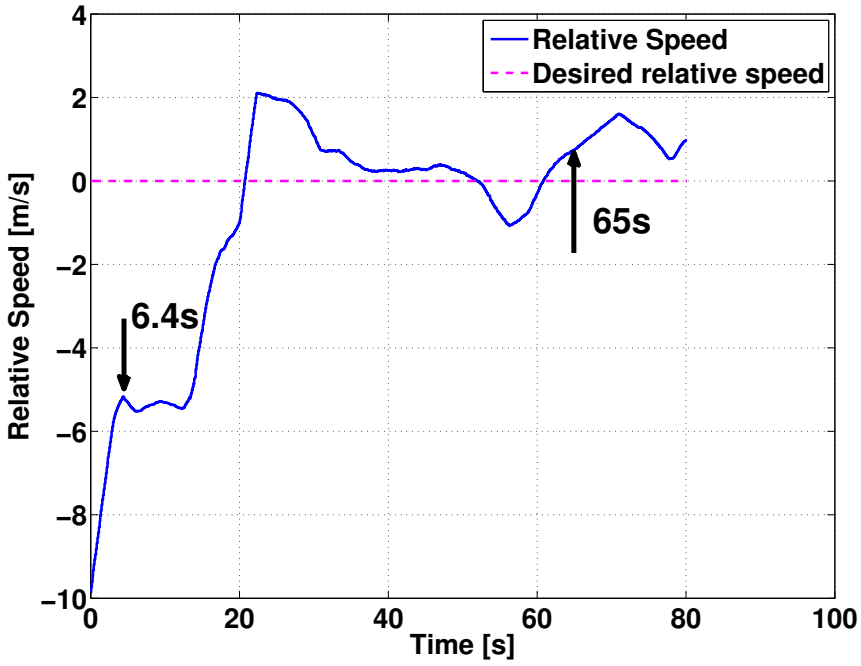

Figure 4.13: Relative Speed

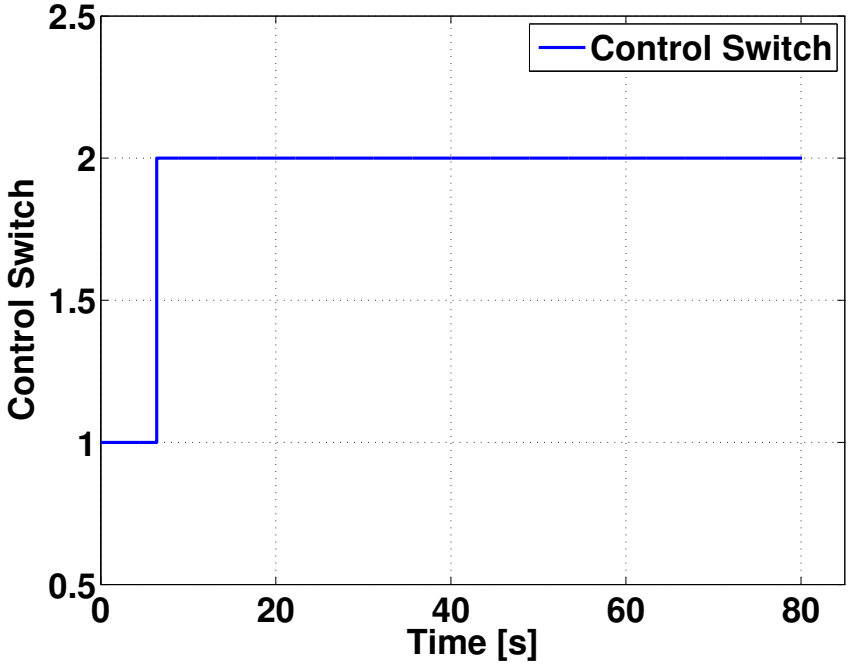

Figure 4.14: Control Switch

the LMPC computes the desired relative acceleration between the following vehicle and the leading vehicle. The assumption of the model is that the position, velocity and acceleration messages can be sent and received through DSRC. But for the experimental results of this work, access to the acceleration of the leading vehicle was not available. There are two possible reasons, one is that the acceleration is not generated from the PinPoint and the other one is the data is failed to send through the DSRC. Because the input of the control system is the relative acceleration, the real model can not match the designed model because of the absence of the acceleration of leading vehicle. Even through the acceleration of leading vehicle is not received, the following vehicle is still following the leading vehicle with the desired distance at the same speed. Additionally, the rapid change of the leading vehicle speed in the test is another potential cause of control error.

4.6.2 Constraints on the Difference of Control Variable

Comparison of Different Constraints on Δu

Another source for the poor performance could be that the desired acceleration is not smooth enough. In the simulation and test, the constraints on the difference of the desired acceleration are $-1.5m/s^2$ and $1.5m/s^2$. Figure 4.15 shows the desired acceleration in the test at a sampling frequency of 1000 Hz. The desired acceleration has many oscillations because of the unsuitable constraints on Δu. The oscillation of the desired acceleration can explain the overshoot of the distance and the error of relative speed. Therefore methods to smooth the desired acceleration should be explored.

The oscillation of the desired acceleration results in the poor performance of the following vehicle. This is one reason that the following vehicle can not follow the leading vehicle very quickly. In order to improve the performance, one solution is to decrease the constraints on the difference of the acceleration. The absolute value of the constraints are set to be $1.5m/s^2$, $0.3m/s^2$, and $0.01m/s^2$. There is more constraint on the difference of the desired acceleration. To validate the changes on the control performance, simulations were run with

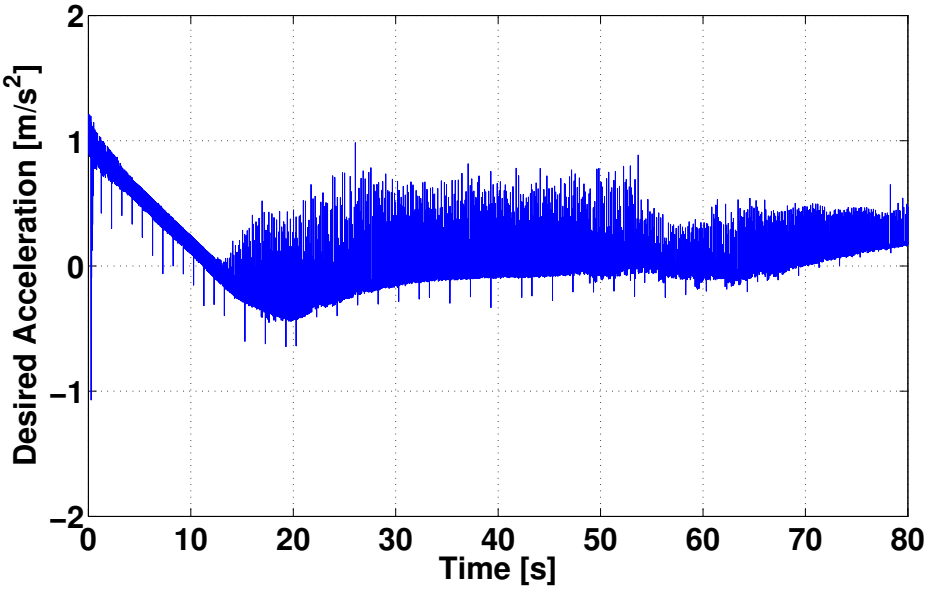

Figure 4.15: Desired Acceleration in the Test

the same weighting matrices defined in Equation (3.45) and Equation (3.46) and the same decay factor($a = 0.5$). The results of the changed acceleration constraints are shown in Figure 4.16 - 4.18.

Comparison of Large Weighting Matrix (R)

Another way to eliminate the oscillations is increase the weighting matrix on the difference of the desired acceleration Δu. This will also have the effect of reducing the constraints of Δu. Figure 4.18 shows that the desired acceleration is smoother without the sacrifice of the control performance. A large weighting matrix ($R = 10000$) is used to improve the smoothess of desired acceleration. The simulation results are shown in Figure 4.19 - 4.22. Figure 4.19 and Figure 4.20 show that the performance of the control system is as same as the performance when $R = 1$. The difference is shown in Figure 4.21, compared to the Figure 4.18. The acceleration almost has no oscillation and is very smooth. Further experimental tests should be performed in the future to validate the controller improvement.

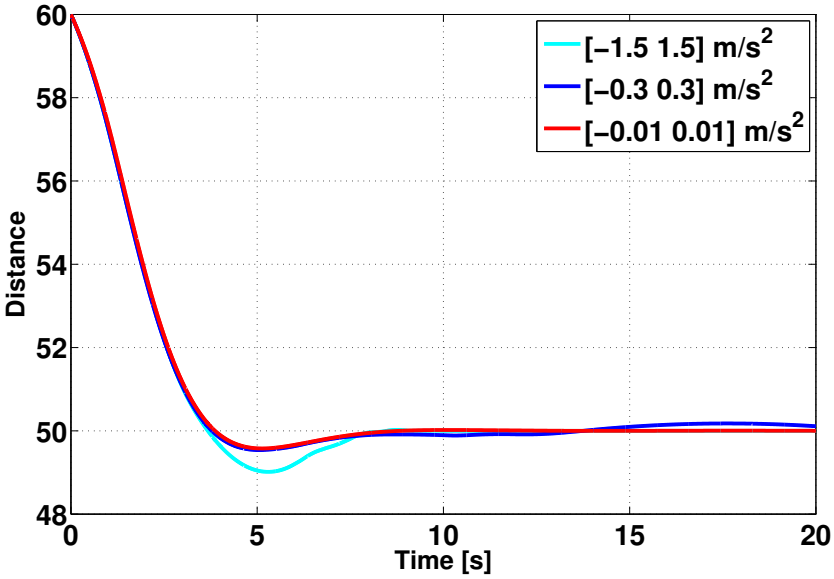

Figure 4.16: Distance

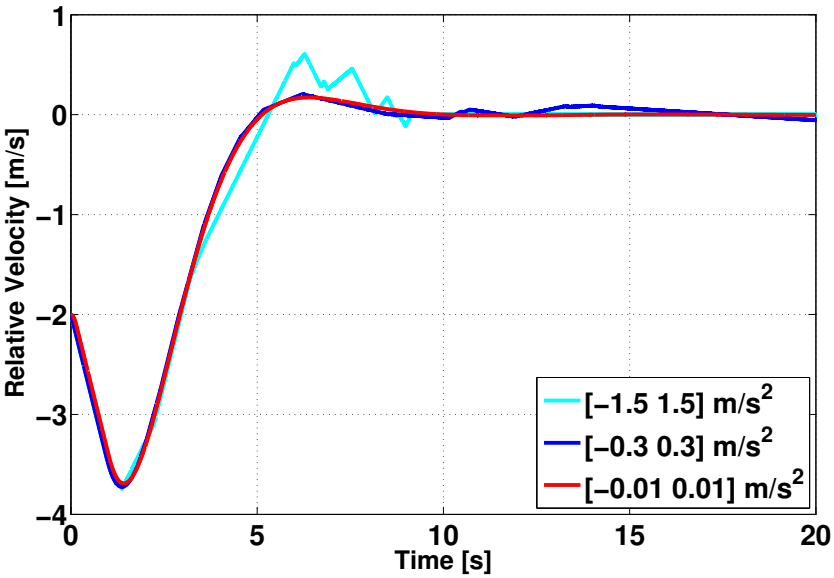

Figure 4.17: Relative Speed

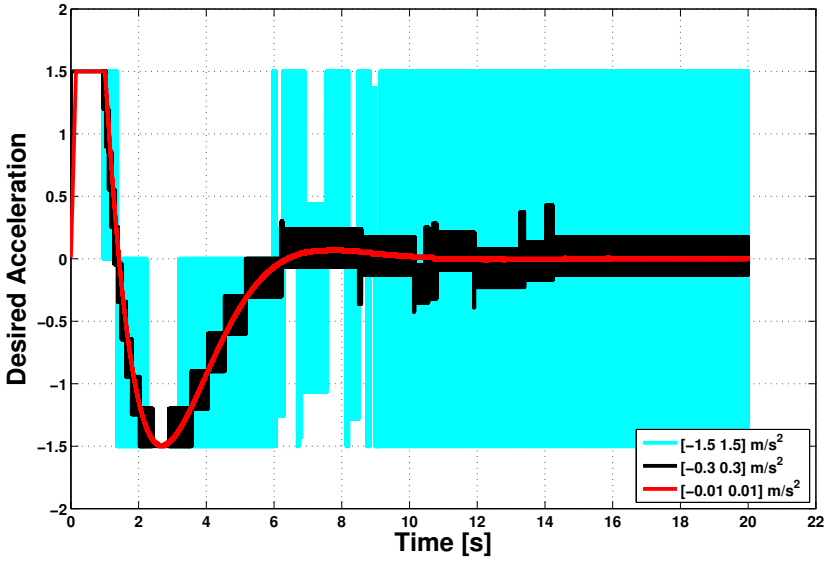

Figure 4.18: Desired Relative Acceleration

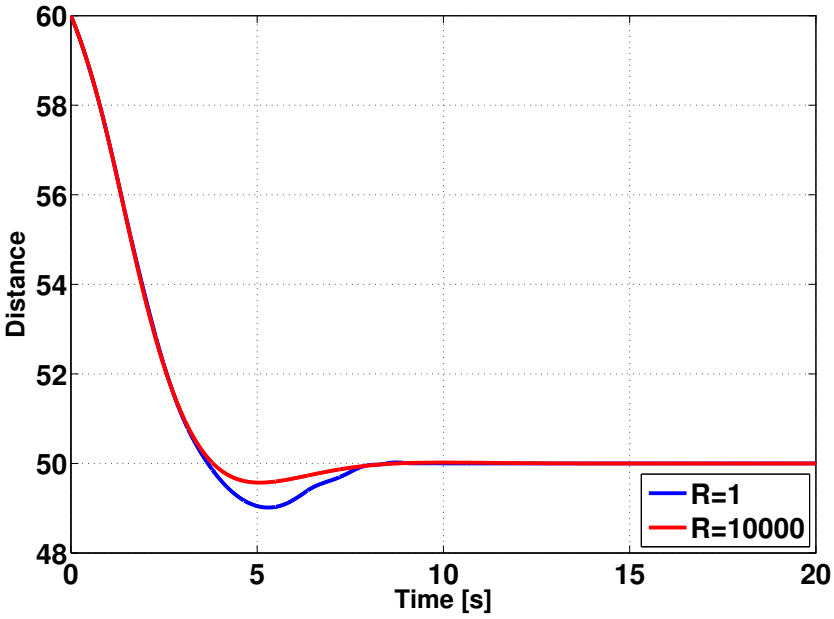

Figure 4.19: Distance

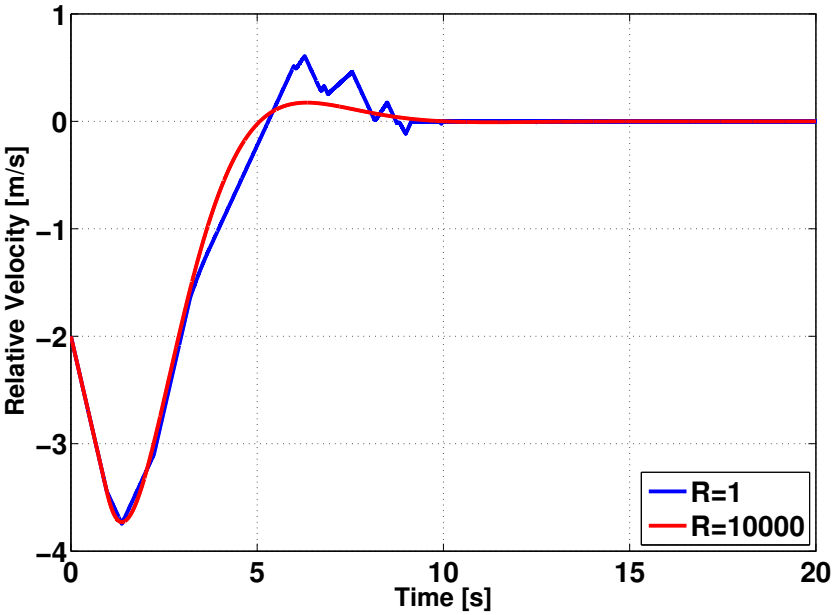

Figure 4.20: Relative Speed

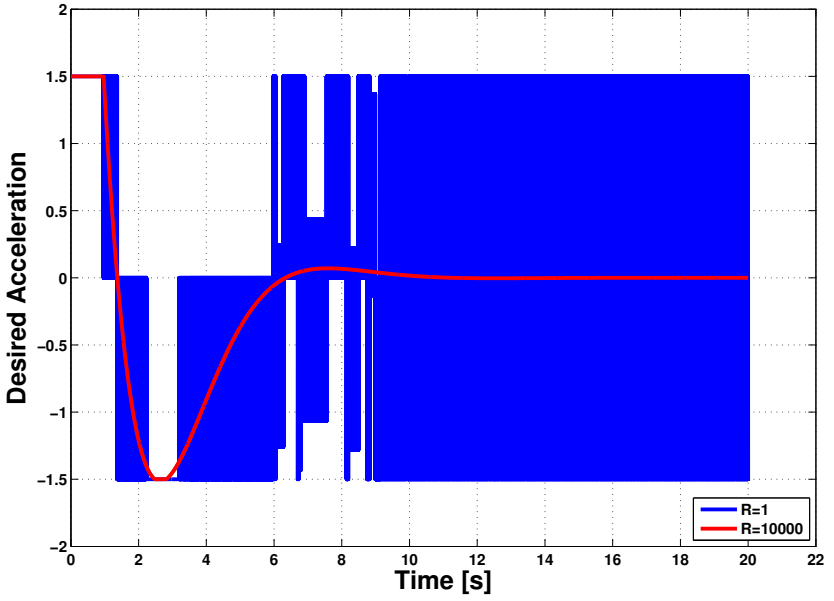

Figure 4.21: Desired Relative Acceleration

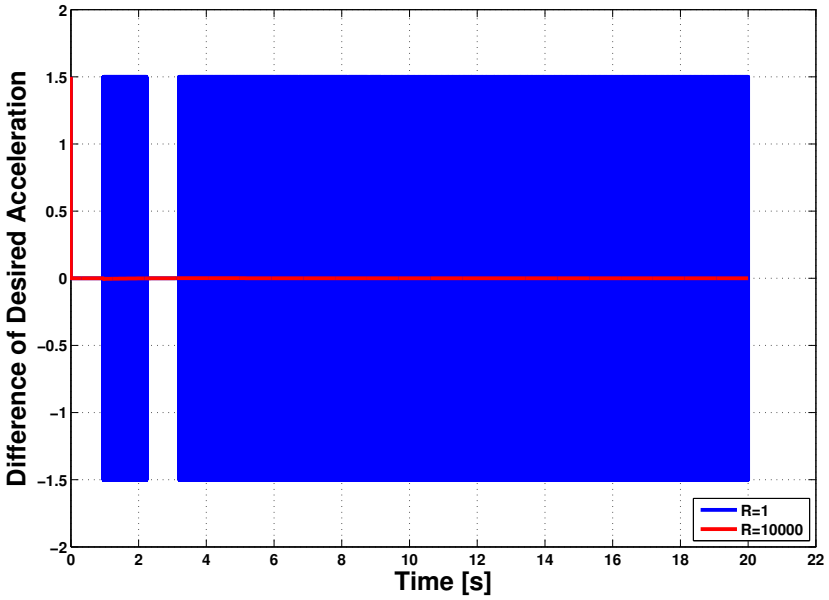

Figure 4.22: Incremental Variation of the Desired Relative Acceleration

4.7 Conclusion

The test equipment, sensors and experiments were discussed in this chapter. The experimental data confirmed the concept of connected vehicle following using the LMPC methods developed in Chapter 3. The vehicles can communicate with each other and share the vehicle information needed for the LMPC control. The control system performed on the experimental platform with overshoot of the actual distance and the speed errors as observed in Figure 4.11 and Figure 4.13. The reasons for the experimental phenomenon were explored and evaluated through the simulations. Two reasons including the absence of the acceleration of leading vehicle and large constraints on the difference of desired acceleration led to the overshoot of distance and the errors of the relative speed. Solutions explored for improving the control performance included reducing the constraints on the difference of the desired acceleration and adjusting the weighting matrix of the control variable. These solutions were validated in simulation and should lead to improved performance of future experiments.

Chapter 5

Conclusion and Future work

This thesis presents the concept of connected vehicles, which can share the vehicle navigation and localization information with the other vehicles. The kinematic relationship of the vehicles involved in the vehicle following maneuver was analyzed. Based on the kinematic equation, the augmented model of vehicle following maneuver and a LMPC were developed to calculate the desired relative acceleration of the following vehicle. Different approximation results were compared by selecting different decay factors (a) of Laguerre functions. Simulations of several model parameters are presented to demonstrate the results. The LMPC algorithm is used as a computational tool to develop a control law for ACC with V2V communication vehicles. A LMPC enabled the control system to be tuned. Performance of closed-loop system was evaluated to show how the control system is tuned by selecting different decay factors. The controller was developed in Simulink and tested on the connected vehicles at Federal Highway Administration (FHWA) Turner-Fairbank Highway Research Center (TFHRC), which had experimental equipment including PinPoint, DSRC, and MicroAutobox. The control algorithm performed fairly well from the simulation results, but the experimental results showed the following vehicle could not follow the leading vehicle very fast. The possible reasons were analyzed. Suggested improvements of the control system were given to improve the performance of the future experiments.

There are many interesting avenues of future work stemming from this thesis. First, performance of the improved controller should be validated. One improvement is to send the acceleration of leading vehicle back to the following vehicle through the DSRC. This will make the designed model in the simulation match with the actual physical vehicle system. Other improvements may be to reduce the constraints on the difference of the desired

acceleration or increase the input weighting matrix. Both constraint reduction and input weighting increase will eliminate the oscillation of the desired acceleration. The experimental performance should be improved with the absence of the oscillated desired acceleration. Second, performance of different control methods such as PID controller, fuzzy-logic control and MPC can be compared through the experimental system. Next, further experimental validation of the different safe distances dependent on different traffic situations should be an objective of the future research. In addition an interesting issue to consider for further research is a comparison of the ACC performance of radar based on relative distance measurement and V2V communication relative distance estimate. Theoretically, connected vehicles can track another vehicle with a closer safe distance, which will improve the traffic flow capacity in the future [28]. Next to these fundamental issues, lane changing and merging of vehicles in everyday traffic present several practical implementation concerns that need to be investigated. With the respect to the lane change and merge concerns, the application of a V2V communication based lateral control system is recommended. Finally, the assumption is that the vehicles are equipped with V2V communication. However in the near future, before all the vehicles have V2V communication, the most important issue for the practical application of automated vehicles is how to resolve interaction of connected and unconnected vehicles.

Bibliography

[1] C. Kreuzen, "Cooperative adaptive cruise control using information from multiple predecessors in combination with MPC," Master of Science Thesis, Delft University of Technology.

[2] Mechanical Simulation, CarSim Overview. Available Online:https://www.carsim.com/products/carsim/ (accessed on 23 September 2015).

[3] B.D.O. Anderson and J. M. Moore. "Linear Optimal Control", Prentice-Hall, Hemel Hempstead, 1971.

[4] James B. Rawlings, David Q. Mayne. Model Predictive Control: Theory and Design. Madison, Wisconsin, 2013.

[5] Liuping Wang. Model Predictive Control System Design and Implementation Using MATLAB. Melbourne, Australia, 2008.

[6] Sinan Oncu, Nathan van de Wouw and Henk Nijmeijer. "Cooperative Adaptive Cruise Control: Tradeoffs Between Control and Network Specification", 2011 14th International IEEE Conference on Intelligent Transportation Systems, 2051-2056, Washington, DC, USA. October 5-7,2011.

[7] MicroAutoBox II Handbook,dSPACE, 2014.

[8] Liuping Wang. "Discrete Time Model Predictive Control Design Using Laguerre Functions", Proceedings of the American Control Conference, Arlington, VA June 25-27, 2001.

[9] Bo Wahlberg. "System Identification Using Laguerre Models",IEEE Transactions on Automatic Control, Vol.36, No.5, May 1991.

[10] PinPoint Localization and Precision IMU User Manual v1.4,TORC Robotics, 2014.

[11] Gerrit Naus, Roel van den Bleek, Jeroen Ploeg, Bart Scheepers, Rene van de Molengraft and Maarten Steinbuch. "Explicit MPC design and performance evaluation of an ACC Stop Go", 2008 American Control Conference, 224-229, Westin Seattle Hotel, Seattle, Washington, USA, June 11-13,2008.

[12] Xiaoyun Lu, J.Karl. Hedrick and Mike Drew. "ACC/CACC-Control Design, Stability and Robust Performance",Proceeding of the American Control Conference, 4327-4332, Anchorage, AK May 8-10, 2002.

[13] Philip D.Olovier. "System Identification Using Laguerre Functions: Sim",Proceeding of the American Control Conference, 4327-4332, Anchorage, AK May 8-10, 2002.

[14] Ten leading causes of injury deaths by age group highlighting unintentional injury deaths, http://www.cdc.gov/injury/wisqars/fatal.html, 2011, accessed: 2015-05-26.

[15] Fatality analysis reporting system:national statistics, http://www-fars.nhtsa.dot.gov/Main/index.aspx, 2012, accessed: 2015-05-26.

[16] A. Vahidi and A. Eskandarian. "Research advances in intelligent collision avoidance and adaptive cruise control". IEEE Transactions on Intelligent Transportation Systems, 4(3):143-153, September 2003.

[17] "Autonomous cruise control", https://en.wikipedia.org/wiki/Autonomous-cruise-control-system, 2013, accessed:2015-09-19.

[18] V. Milane's, M. Marouf, J. Pe'rez, D. Gonza'lez, and F. Nashashibi, "Low-speed cooperative car-following fuzzy controller for cybernetic transport systems," in Intelligent Transportation Systems (ITSC), 2014 IEEE 17th International Conference on. IEEE, 2014, pp. 2075?2080.

[19] R. Kianfar, B. Augusto, A. Ebadighajari, U. Hakeem, J. Nilsson, A. Raza, R. S. Tabar, N. Irukulapati, C. Englund, P. Falcone et al., "Design and experimental validation of a cooperative driving system in the grand cooperative driving challenge," Intelligent Transportation Systems, IEEE Transactions on, vol. 13, no. 3, pp. 994-1007, 2012.

[20] Khaled Sailan and Klaus.Dieter Kuhnert, "Modeling and design of cruise control system with feedforward for all terrain vehicles," Computer Science and Information Technology, pp. 339-349, 2013.

[21] Connected Vehicles DSRC Frequently Asked Questions, USDOT Research and Innovation Technology Administration (RITA), ITS Joint Program Office, http://www.its.dot.gov/DSRC/dsrc-faq.htm

[22] Gerrit J.I Naus Ploeg, M.J.G.(Rene) Van de Molengraft, W.P.M.H.(Maurisce) Heemels and Maarten Steinbuch."A Model Predictive Control Approach to Design a Parameterized Adaptive Cruise Control", Lecture Notes in Control and Information Sciences.

[23] Dik de Bruin, Joris Kroon, Richard van Klaveren and Martin Nelisse. "Design and Test of a Cooperative Adaptive Cruise Control System", 2004 IEEE Intelligent Vehicles Symposium, University of Parma, Parma, Italy, June 14-17,2004.

[24] Seungwuk Moon, Kyongsu Yi and Ilki Moon. "Design, Tuning and Evaluation of Integrated ACC/CA System", Proceedings of 17th world Congress, The International Federation of Automatic Control, Seoul, Korea, July 6-11,2008.

[25] Feyyaz Emre Sancar, Baris Fidan, Jan P. Huissoon and Steven L. Waslander. "MPC Based Collaborative Adaptive Cruise Control with Rear End Collision Avoidance", 2014 IEEE Intelligent Vehicles Symposium (IV) June 8-11,2014,Dearborn, Michigan, USA.

[26] Vibhor L.Bageshwar, William L. Garrard, and Rajesh Rajamani, "Model Predictive Control of Transitional Maneuvers for Adaptive Cruise Control Vehicles", IEEE Transactions on Vehicular Technology, Vol.53,No.5,Septemper 2004.

[27] D.Corona, I,Necoara,B.De Schutter and T. van den Boom, "Robust hybrid MPC applied to the design of an adaptive cruise controller for a road vehicle,"Proceedings of the 45th IEEE Conference on Decision and Control, San Diego, California,pp.1721-1726,Dec.2006.

[28] Joel VanderWerf, Steven E.Shladover, Mark A. Miller and Natalia Kourjanskaia,"Effects of Adaptive Cruise Control Systems on Highway Traffic Flow Capacity", Transportation Research Record 1800, Paper No.02-3665.

[29] Ching-Yao Chan, "Connected vehicles in a connected world", Automation and Test (VLSI-DAT), 2011 International Symposium on. IEEE, 2011.

[30] Jyongsu Yi, Youngjoo Cho, Sejin Lee, Joonwoong Lee and Namkyoo Ryoo, "A Throttle/Brake Control Law for Vehicle Intelligent Cruise Control", Seoul 2000 FISITA World Automotive Congress, June 12-15, 2000,Seoul, Korea.

[31] Fanping Bu, Han-Shue Tan and Jihua Huang, "Design and Field Testing of A Cooperative Adaptive Cruise Control System", 2010 American Control Conference, Marriott Waterfront, Baltimore, MD, USA, June 30-July 02,2010.

[32] Jeroen Ploeg, Bart T.M.Scheepers, Ellen van Nunen, Nathan van de Wouw and Henk Nijmeijer, "Design and Experimental Evaluation of Cooperative Adaptive Cruise Control", 2011 14th International IEEE Conference on Intelligent Transportation Systems, Washington, DC, USA.

[33] Vicente Milanes, Steven E. Shladover, John Spring, Christopher Nowakowski, hiroshi Kawazoe and Masahide Nakamura, "Cooperative Adaptive Cruise Control in Real Traffic Situations", IEEE Transactions on Intelligent Transportation Systems, Vol.15, No.1, February 2014.

[34] Yue Yu, Abdelkader El Kamel and Guanghong Gong, "Modeling and simulation of overtaking behavior involving environment", Advances in Engineering Software 67 (2014) 10-21.

[35] Martin Treiber, Ansgar Hennecke and Dirk Helbing."Congested Traffic States in Empirical Observations and Microscopic Simulations", arXiv:cond-mat/0002177v2 [cond-mat.stat-mech] 30 Aug 2000.

[36] P.Ioannou and Z.Xu."Throttle and Brake Control Systems for Automatic Vehicle Following", University of Southern California, California PATH Research Paper, April 1994.

[37] Paolo Caravani, Elena De Santis, Fabio Graziosi and Emanuele Panizzi."Communication Control and Driving Assistance to a Platoon of Vehicles in Heavy Traffic and Scarrce

Visibility", IEEE TRANSACTIONS ON INTELLIGENT TRANSPORTATION SYSTEMS,VOL. 7, NO. 4, DECEMBER 2006.

[38] R. Hallouzi, V.Verdult, H. Hellendoorn, P.L.J.Morsink and J.Ploeg."Communication based Longitudinal Vehicle Control Using an Extended Kalman Filter", TNO report, TNO Automative, Advanced Chassis and Transport Systems, Netherlands.

[39] R.Hallouzi, V.Verdult, H.Hellendoorn and J.Ploeg."Experimental Evaluation of a Cooperative Driving Setup based on Inter-Vehicle Communication", TNO report, TNO Automative, Advanced Chassis and Transport Systems, Netherlands.

[40] Mohsen Padash, Mahdi Tavassoli, Abdullah Khoei and Khayrollah Hadidi,"A Sophisticated Algorithm for Using Fuzzy Logic Controllers in Adaptive Cruise Controller Systems", Universal Journal of Electrical and Electronic Engineering 1(4):134-141,2013.

[41] S. Cloudin and K. Komathy,"Performance Analysis of Fuzzy Cooperative Adaptive Cruise Controller in Vehicular Ad-hoc Networks", Chennai Fourth International Conference on Sustainable Energy and Intelligent Systems (Section 2013) 12-14 Dec 2013.

[42] S.Paul Sathiyan and A.Wisemin Lins,"Soft Computing based Adaptive Cruise Control", India Journal of Computer Science and Engineering, Vol.2 No.1.

[43] Shengbo Li, Keqiang Li, Rajesh Rajamani, and Jianqiang Wang,"Model Predictive Multi-Objective Vehicular Adaptive Cruise Control", IEEE Transactions on Control Systems Technology, Vol.19, No.3, May 2011.

[44] G. Valencis-Palomo and J.A. Roster,"Using Laguerre functions to improve efficiency of multi-parametric predictive control", 2010 American Control Conference, Marriott Waterfront, Baltimore, MD, USA, June-30-July 02, 2010.

[45] Vicente Milanes, Mohamed Marouf, Joshue Perez, David Gonzalez and Fawzi Nashsshibi,"Low-speed Cooperative Car-Following Fuzzy Controller for Cybernetic Transport Systems", 2014 IEEE 17th International Conference on Intelligent Transportation Systems (ITSC) October 8-11, 2014. Qingdao, China.

[46] Nasser Saghatoleslami, and Masood Khaksar Toroghi,"Controlling Nonlinear Processes, using Laguerre Functions Based Adaptive Model Predictive Control (AMPC) Algorithm", Journal of Chemical and Petroleum Engineering, University of Tehran, Vol. 45, No. 1, June, 2011, PP. 47-55.

[47] Vicente Milanes, Mohamed Marouf, Joshue Perez, David Gonzalez and Fawzi Nashsshibi,"Low-speed Cooperative Car-Following Fuzzy Controller for Cybernetic Transport Systems", 2014 IEEE 17th International Conference on Intelligent Transportation Systems (ITSC) October 8-11, 2014. Qingdao, China.

[48] J.A. Rossiter, L.Wang and G. Valencia-Palomo,"Efficient algorithm for trading off feasibility and performance in predictive control", International Journal of Control, Vol. 83, No.4, April 2010, 789-797.

[49] J.A. Rossiter, L.Wang and G. Valencia-Palomo,"Exploiting Laguerre functions to improve the feasibility/performance compromise in MPC", Decision and Control, 2008. CDC 2008. 4th IEEE Conference.

[50] Mange Sudhakara and Abraham T Mathew,"Moel Predictive Control using Laguerre Functions for Ship Heading Control with I/O",International Journal on Theoretical and Applied Research in Mechanical Engineering.

[51] Milu Solaman and Roya mary Francis,"Model Predictive Controller Based on Laguerre Function for Binary Distillation Column",International Journal of Scientific Engineering and Research, Volume 3 Issue 8, August 2015, 2347-3878.

[52] G. Valencia-Palomo, J.A. Rossiter, C.N. Jones, R. Gondhalekar and B. Khan ,"Alternative parameterisations for predictive control: how and why?", 2011 American Control Conference on O'Farrell Street, San Francisco, CA, USA, June 29-July 01, 2011.

[53] B.Khan and J.A.Rossiter ,"A comparison of the computational efficiency of generalized function MPC using active set methods", Preprints of the 8th IFAC Symposium on Advanced Control Chemical Process The International Federation of Automatic Control Furama Riverfront, July 10-13, 2012.

[54] R.C. Gutierrez-Urquidez, G. Valencia-Paloma, O.M. Rodriguez-Elias and L.Trujillo,"Systematic selection of tuning parameters for efficient predictive controllers using a multi objective evolutionary algorithm", Applied Soft Computing 312 (2015) 326-338.

Appendices

Appendix A

Notes on the style-file project